

5-2011

Lateral variability of facies and cycles in the Furongian (Late Cambrian) Carbonate Platform: An example from the Big Horse Member of the Orr Formation in western Utah, U.S.A.

Ratna Widiarti
University of Nevada, Las Vegas

Follow this and additional works at: <https://digitalscholarship.unlv.edu/thesesdissertations>



Part of the [Geology Commons](#), [Sedimentology Commons](#), and the [Stratigraphy Commons](#)

Repository Citation

Widiarti, Ratna, "Lateral variability of facies and cycles in the Furongian (Late Cambrian) Carbonate Platform: An example from the Big Horse Member of the Orr Formation in western Utah, U.S.A." (2011). *UNLV Theses, Dissertations, Professional Papers, and Capstones*. 1005.
<http://dx.doi.org/10.34917/2349464>

This Thesis is protected by copyright and/or related rights. It has been brought to you by Digital Scholarship@UNLV with permission from the rights-holder(s). You are free to use this Thesis in any way that is permitted by the copyright and related rights legislation that applies to your use. For other uses you need to obtain permission from the rights-holder(s) directly, unless additional rights are indicated by a Creative Commons license in the record and/or on the work itself.

This Thesis has been accepted for inclusion in UNLV Theses, Dissertations, Professional Papers, and Capstones by an authorized administrator of Digital Scholarship@UNLV. For more information, please contact digitalscholarship@unlv.edu.

LATERAL VARIABILITY OF FACIES AND CYCLES IN THE FURONGIAN
(LATE CAMBRIAN) CARBONATE PLATFORM: AN EXAMPLE FROM
THE BIG HORSE MEMBER OF THE ORR FORMATION IN
WESTERN UTAH, U.S.A.

by

Ratna Widiarti

Bachelor of Science
Institute of Technology Bandung
2008

A thesis submitted in partial fulfillment of
the requirements for the

Master of Science in Geoscience
Department of Geoscience
College of Science

Graduate College
University of Nevada, Las Vegas
May 2011

Copyright by Ratna Widiarti 2011
All Rights Reserved



THE GRADUATE COLLEGE

We recommend the thesis prepared under our supervision by

Ratna Widiarti

entitled

Lateral Variability of Facies and Cycles in the Furongian (Late Cambrian) Carbonate Platform: An Example from the Big Horse Member of the Orr Formation in Western Utah, U.S.A.

be accepted in partial fulfillment of the requirements for the degree of

Master of Science in Geoscience

Ganqing Jiang, Committee Chair

Stephen M. Rowland, Committee Member

Andrew Hanson, Committee Member

Felicia F. Campbell, Graduate Faculty Representative

Ronald Smith, Ph. D., Vice President for Research and Graduate Studies
and Dean of the Graduate College

May 2011

ABSTRACT

Lateral Variability of Facies and Cycles in the Furongian (Late Cambrian) Carbonate Platform: An Example from the Big Horse Member of the Orr Formation in Western Utah, U.S.A.

by

Ratna Widiarti

Dr. Ganqing Jiang, Examination Committee Chair
Associate Professor of Geoscience
University of Nevada, Las Vegas

Carbonate depositional cycles and sequences have been proposed to be formed by glacioeustatic sea-level changes. This mechanism would be questionable during times of high atmospheric CO₂ and negligible continental ice sheets such as the supergreenhouse time in the Furongian (late Cambrian), during which limited glacioeustatic sea-level changes would be expected. A detailed sedimentological study of the Furongian Orr Formation in western Utah is aimed at testing the hypothesis that, under supergreenhouse climate conditions, most meter-scale carbonate cycles may have been formed through autocyclic processes and thus they should be laterally variable. The research was conducted in a small area (< 1.2 km²) where excellent exposure permits lateral tracing of key surfaces and facies.

The Big Horse Member of the Orr Formation in the study area mainly consists of shale, siltstone, cryptic microbialites, thrombolites, wackestone, and cross-laminated oolitic grainstone/packstone that were deposited from deep subtidal to supratidal environments. Meter-scale cycles are expressed by shallowing-upward trends with subtidal shale/siltstone at the base and supratidal microbialites with desiccation cracks, dissolution cavities, and karstic breccias at the top. Among the seven closely-spaced

sections with traceable marker beds, the cycle numbers vary and the thickness of individual cycles change from 2 m to 36 m. Individual cycles are found to change within a few hundreds of meters to non-cyclic interval or, in some cases, several cycles merge into a single cycle within 200-1100-meter distance. However, two stratigraphic discontinuities marked by intensive subaerial exposure were traceable among sections. These features suggest that meter-scale cycles of the Big Horse Member were mainly formed by autocyclic process through interactions among tidal island aggradation, local carbonate production rates, and tectonic/thermal subsidence. Forced regression during times of high carbonate production formed the laterally persistent discontinuities, but their duration may have varied, with significant lag time recorded in some sections.

TABLE OF CONTENTS

ABSTRACT	iii
LIST OF FIGURES	vi
ACKNOWLEDGEMENT	vii
CHAPTER 1 INTRODUCTION	1
CHAPTER 2 GEOLOGICAL BACKGROUND AND STRATIGRAPHY	4
2.2 Stratigraphy of the Orr Formation	5
2.3 Previous Work	6
CHAPTER 3 METHODS	7
CHAPTER 4 FACIES AND DEPOSITIONAL ENVIRONMENTS	9
4.1 Deep Subtidal Facies Association (FA-1).....	9
4.2 Shallow Subtidal Facies Association (FA-2).....	10
4.3 Peritidal Microbial Facies Association (FA-3).....	12
4.4 Subaerial Exposure Facies Association (FA-4).....	14
4.5 Evolution of Depositional Environments.....	15
CHAPTER 5 CYCLES AND CYCLE VARIATIONS.....	17
5.1 Cycle Definition and Cycle Types.....	17
5.1.1 Microbialite-rich Peritidal Cycles.....	18
5.1.2 Thrombolite-capped Cycles.....	20
5.1.3 Grainstone/packstone-capped Subtidal Cycles.....	21
5.2 Temporal and Spatial Variation of Cycles.....	21
CHAPTER 6 DISCUSSIONS	23
6.1 Formation of Meter-scale Cycles.....	23
6.2 Implications for Cyclostratigraphy in Greenhouse Carbonate Platforms.....	25
CHAPTER 7 CONCLUSIONS	27
TABLES AND FIGURES	28
REFERENCES	52
VITA.....	58

LIST OF FIGURES

Figure 1	A google image and map showing the location of study area in the Little Horse Canyon, western Utah.	31
Figure 2	Stratigraphic column of the Orr formation in House Range, western Utah....	32
Figure 3	Stratigraphic column from seven sections of the upper Big Horse Member in the Little Horse Canyon, western Utah.....	33
Figure 4	Lateral facies variations of the studied interval within the Big Horse Member.....	34
Figure 5	Generalized depositional model and the distribution of lithofacies and facies associations in the Big Horse Member.....	35
Figure 6	Field and petrographic photos of deep and shallow subtidal facies associations.....	37
Figure 7	Field and petrographic photos of the shallow subtidal facies association.....	38
Figure 8	Field and petrographic photos of the peritidal microbial facies association...	41
Figure 9	Subaerial exposure features.....	42
Figure 10	Schematic temporal evolution of depositional environments.....	44
Figure 11	Representative meter-scale cycles from the Big Horse Member of the Orr Formation, Little Horse Canyon, western Utah.....	46
Figure 12	Field view of cycles in section BH7.....	47
Figure 13	Correlation panel of carbonate cycles in sections BH6 and BH7.....	47
Figure 14	Tracing of carbonate cycles from section BH2 to BH3.....	48
Figure 15	Lateral variability of cycles in the uppermost 40 meters of the studied interval.....	49
Figure 16	An example showing the formation of microbialite-rich peritidal cycles.	50
Figure 17	Schematic diagram showing the autogenic origin of cycles and their lateral variations.....	51

ACKNOWLEDGEMENT

Primarily, I would like to thank my advisor, Dr. Ganqing Jiang (GQ), for supporting me to complete this thesis. I was grateful to have him as my advisor, who was able to keep in touch anytime and to provide feedbacks and everlasting motivations. I would never forget his kind heart to assist me achieving my academic goals. Secondly, I was grateful to have Prof. Dr. Stephen (Steve) Rowland, Dr. Andrew Hanson, and Prof. Dr. Felicia Campbell (Dr. C) as my committee members. They were all supportive in helping me to complete my project with constructive evaluations. Thank you to Dr. Margaret (Peg) Rees for sharing the expertise during fieldwork in Nevada and Utah. It was wonderful experience to be a part of Department of Geoscience UNLV, with amazing faculty members and department staffs. Thanks also to Nicholle Booker for the helping me to accomplish graduate documents. Special thanks goes to my fellow “Carbonate Mafia” (Adam Zeiza, Swapan Sahoo, Jon Baker, and Bobby Henry), to whom I owed a lot and could not think I would be able to return. Without their help, I could not have completed this thesis. Thank you to all Indonesian students for the happy time (Yuki, Laode, Leon, George, Ynnez), they were such my sisters and brothers here. Special thanks to Geoscience fellow students, especially who attended Fall 2008 semester and my office mates. Last but not least, I wish to thank my family (Hari Susilo, Sudarti, and Retno) and Fikry for their never-ending supports and prayers.

This thesis was made possible through a full funding from ExxonMobil Oil Indonesia and assistance from ExxonMobil Houston. Special thanks to Institute of International Education (IIE) for managing my student requirements and international affairs.

CHAPTER 1

INTRODUCTION

Carbonate cycles and sequences in sedimentary successions, particularly those from passive continental margins, have been interpreted as having formed by glacioeustatic changes (i.e., Haq et al., 1987; Loucks and Sarg, 1993; Haq and Schutter, 2008; Lukasik and Simo, 2008). This is possibly true for icehouse times when high-latitude and polar ice sheets were present. Cycles and sequences formed by glacioeustatic sea-level changes presumably have high lateral continuity and thus are correlatable across continental shelves and sedimentary basins (Grotzinger, 1986; Goldhammer et al., 1993; Lehrmann and Goldhammer, 1999). However, during supergreenhouse times when high atmospheric CO₂ (>2000 ppm, for example) prevented the development of polar ice sheets (i.e., Berner, 2003), the driving mechanisms for sedimentary cyclicity remain unclear.

Without significant glacioeustatic sea-level change during supergreenhouse times, the major difficulty to develop sedimentary cycles is the repetitive generation of accommodation space required for sediment accumulation (De Benedicts et al., 2007). Tectonic subsidence may provide long-term accommodation space, but because carbonate sedimentation rate often exceeds tectonic subsidence in passive continental margins, greater facies migration and more frequent stratigraphic discontinuities may be expected (Lehrmann and Goldhammer, 1999). In such conditions, autocyclicity may be more common due to forced regression at local scales (Pratt and James, 1986; Adams and Grotzinger, 1996; Booler and Tucker, 2002; Sarg et al., 1999; Lehrmann et al., 2007). Because the creation of accommodation space through interactions between carbonate

production and tectonic subsidence may not be as regular as that by glacioeustatic sea-level changes, carbonate cycles and sequences formed during supergreenhouse times may display greater temporal variations in cycle thickness and duration.

The Furongian (late Cambrian) is one of the supergreenhouse times in Earth history, during which atmospheric CO₂ level is inferred to have been as high as > 4000 ppm (Bernier, 2003) and no glacial record has been found, possibly due to high temperature in Earth's surficial environments. It is thus an important time interval to test the expression and lateral variations of carbonate cycles formed in a supergreenhouse climate. Particularly during the Furongian, the western United States represents a carbonate platform developed over a stable passive continental margin where the tectonic subsidence rate is relatively easy to quantify, giving a great opportunity to investigate the cycle patterns and their potential driving mechanisms.

In this research, a detailed sedimentological study of the early Furongian carbonate platform in western Utah was conducted to reveal the carbonate cycles, their vertical stacking patterns and lateral variations so that a better understanding of the cycle-controlling mechanisms during supergreenhouse climate can be achieved. Fieldwork was focused on the Big Horse Member of the Orr Formation in Little Horse Canyon of western Utah (Figure 1) where excellent exposure allows tracing individual facies and cycles at walkable distances.

The Big Horse Member in the study area is about 220 m thick, and the studied interval belongs to the middle part of the Big Horse Member (Fig. 2). The uppermost datum (S1) used in the studied interval is 82 m below the boundary between the Big Horse Member and the overlying Candland Shale. Because the contact between the Big

Horse Member and its underlying Weeks Limestone is covered, sections were measured downward from the upper datum until outcrop exposure did not permit lateral tracing of facies and cycles.

CHAPTER 2

GEOLOGICAL BACKGROUND AND STRATIGRAPHY

2.1 Tectonics

Cambrian strata of western North America were deposited on a passive continental margin that was developed over the rift associated with the breakup of supercontinent Rodinia during the late Neoproterozoic (Bond et al., 1983; Dickinson, 2006). By middle Cambrian time (Cambrian Series 3), a northwest-facing carbonate platform covered most of present-day Utah, Nevada, and southeastern California. Across the carbonate platform, fine-grained terrigenous sediments accumulated in deep-water environments towards the west in California and carbonate-rich sediments dominated in shallow-water environments east of Tonopah, Nevada (Palmer, 1971; Cook and Corboy, 2006). This stratigraphic pattern was disrupted during the Stage 5 or the *Ehmaniella* trilobite zone by the development of a syndepositional, fault-controlled intrashelf basin known as the House Range Embayment (Rees, 1986). Syndepositional fault activity within the House Range Embayment is inferred to have started during the latest *Ehmaniella* trilobite zone (Rees, 1986; Howley and Jiang, 2010) and the fault-controlled accommodation was filled by the end of Stage 7 (*Cedaceria-Crepichepalus* trilobite zones). Episodic fault reactivation within the House Range Embayment may have happened during Furongian, and the final phase of fault-related accommodation was filled by the end of the Cambrian (Evans, 1997).

2.2 Stratigraphy of the Orr Formation

In Little Horse Canyon, the Furongian Orr Formation consists of, in ascending order, the Big Horse Member, the Candland Shale Member, the Johns Wash Limestone Member, the Corset Spring Shale Member, and the Sneakover Limestone Member (e.g., Ludvigsen and Westrop, 1985), with a total thickness of 392-453 meters (Hintze and Robison, 1975 Figure 2). The Orr Formation is overlain by the Ordovician Notch Peak Formation that consists of ~520m of massive limestone and dolostone with abundant microbialites and domal stromatolites/thrombolites. Underlying the Orr Formation is the Cambrian Series 3 Weeks Limestone, which shows a shallowing-upward sequence recording the filling history of the fault-controlled Horse Range Embayment (Rees, 1986). The boundary between the Orr Formation and the Weeks Limestone is not clear in the study area.

The Big Horse Member is composed of shallow-water carbonates that mark the end of the first phase of tectonic subsidence within the House Range Embayment. Syndepositional fault activities may have rejuvenated thereafter, associated with the deposition of subtidal shale and carbonates of the Candland Shale Member and the Corset Spring Shale Member, respectively. The top of the Notch Peak Formation is characterized by a regionally consistent karstic unconformity, marking the end of the House Range Embayment (Evans et al., 2003). The focus interval of this study is the middle part of the Big Horse Member (Figure 2).

2.3 Previous Work

The Big Horse Member is equivalent with the *Crepicephalus* trilobite zone, which occurred in early Furongian or at around the boundary of Cambrian Series 3 and Furongian. It consists of shallow subtidal to peritidal carbonates and shales that display cyclic patterns. Previous work reported six shallowing-upward cycles within the Big Horse Member (Lohmann, 1977 cited in Hover-Granath et al., 1983). The base of each cycle consists of interbedded mudstones-wackestones and terrigenous siltstones, while the upper part consists of algal boundstone or oolitic grainstone (Hover-Granath et al., 1983). More meter-scale cycles have been reported in later studies, and they were interpreted as having formed by glacioeustatic sea-level changes controlled by Milankovitch astronomical forcing (Osleger and Read, 1991). Cycles were thought to be regionally correlatable across the Furongian carbonate platform in the Great Basin, although the authors noted that the expression and thickness of these cycles vary among widely separated sections (Osleger and Read, 1991).

CHAPTER 3

METHODS

Seven closely spaced sections in the Little Horse Canyon were studied to construct a detailed meter-scale sedimentological framework (Figures 1 and 3). The thickness each section was measured bed by bed using a Jacob staff that was put perpendicular to the bedding planes. Facies and cycles were identified within each section, and then they were traced laterally between sections.

Lithofacies and facies associations were identified from field observations on the basis of sedimentary structures, textures, bedding contact, and their vertical and lateral variations. Fifty-three samples were chosen to make petrographic thin sections in order to examine and confirm (1) the texture and constituents of representative facies and (2) diagenetic features at exposure surfaces (cycle boundaries).

Thirteen lithofacies have been identified from the Big Horse Member in the study area. Their composition, bedding contacts, sedimentary structures and textures are summarized in Table 1. These facies are grouped into four facies associations, including deep subtidal (FA-1), shallow subtidal (FA-2), peritidal microbial (FA-3), and subaerial exposure facies associations (FA-4). The vertical stacking patterns (cycles) of these facies/facies associations are provided in seven representative sections (Figure 3) and their lateral variability and depositional environments are given in Figure 4. The studied interval includes a number of facies developed in a ramp tidal system, from deep subtidal to supratidal areas. A generalized depositional model for these facies/facies associations is provided in Figure 5. Representative photographs for each facies association are

provided in Figures 6 to 9, and evolution of depositional environments is provided in Figure 10.

A large portion of the efforts during the fieldwork was focused on defining and tracing the cycles and their temporal/lateral variations. Examples of such efforts are provided in Figures 11-15. The exposure in the western ridge complex allowed lateral physical tracing of facies and surfaces (S1-S3) between the five western sections (BH1, BH2, BH3, BH4, and BH5). However, the correlation between these sections and the other two eastern sections (BH6 and BH7) was based on the top surface (S1) and the existence of cycle top and exposure surfaces at approximately the same level in each section (Figures 3-4). The three surfaces (S1, S2, and S3) divided the studied stratigraphic interval into three parts (Figures 4), and the cycle types and formation mechanisms may have been slightly different, as shown in Figures 16 and 17.

CHAPTER 4

FACIES AND DEPOSITIONAL ENVIRONMENTS

4.1 Deep Subtidal Facies Association (FA-1)

The deep subtidal facies association includes two facies: (1) interbedded calcareous shale, and (2) silty limestone and mixed shale and limestone. These facies are most common in the lower part of measured sections (Figures 3 and 4) and commonly form the lower part of shallowing-upward cycles that are capped by shallow subtidal grainstone/packstone facies (e.g., Figure 6a).

Interbedded calcareous shale and silty limestone commonly form shale-carbonate couplets of uneven thickness. In most cases silty limestone beds are 2-5 cm thick and the shale interbeds are from a few millimeters to 3 cm thick (Figure 6a and d). Silty limestone layers are laterally continuous, showing millimeter-thick parallel laminations (Figure 6d), and small-scale wavy cross-laminations. Due to compaction, calcareous shale layers are often discontinuous and chertified (Figure 6e), while the silty limestone layers form nodular structures (interval A in Figure 6e).

The mixed shale and limestone facies is characterized by relatively thicker shale intervals with thin lime mudstone-wackestone interbeds (e.g., the lower part of measured sections; Figure 3). The limestone layers contain bioclasts, peloids, and oncoids (Figure 6c). Occasionally fine-grained peloidal grainstone beds with minor erosional surfaces at the base are present. Parallel laminations are common in shales, sometimes with bioturbation and burrows appearing on bedding surfaces.

These two facies are interpreted to have been deposited from deep subtidal environments below fair-weather wave base (Figure 5). An abundance of parallel

laminations in shales indicates suspension deposits in low-energy environments. The presence of subordinate grainstone/packstone layers (e.g., interval B in Figure 6a) suggests either episodic shoaling towards shallow-subtidal environments or deposition from storm events that bring coarse-grained sediments from shallow- to deep-water environments.

4.2 Shallow Subtidal Facies Association (FA-2)

The shallow subtidal facies association consists of oolitic-oncolitic packstone, oolitic-bioclastic packstone/grainstone, and cross-bedded oolitic-bioclastic packstone/grainstone. These facies are present as thin beds within shale-dominated intervals or as thick and laterally discontinuous units (Figures 3 and 4). In the lower part of measured sections (Figures 3 and 4), these facies commonly form the upper part of the meter-scale cycles overlying the deep subtidal facies association (i.e., Figure 6a). In some cases, thin shaly layers or lenses are present between packstone/grainstone beds (e.g., Figure 6b, e, and f), demonstrating the transition from deep subtidal, shale-dominated facies to shallow subtidal, packstone/grainstone-dominated facies.

The oolitic-oncolitic packstone facies is commonly present in the lower part of measured sections and consist of thin mud drapes between beds (e.g., Figure 6b, interval B in 6e, and 6f). Individual packstone layers are 2-10 cm thick, with ripple cross laminations in some intervals (e.g., Figure 6f). The presence of laterally discontinuous mud drapes indicates alternating high- and low-energy conditions. This facies is interpreted as deposition in shallow subtidal environments slightly above or close to the

fair-weather wave base, where frequent changes between high- and low-energy conditions may occur.

The presence of oolitic-bioclastic packstone/grainstone facies is similar to that of the oolitic-oncolitic packstone. This facies occurs mostly in the lower part of measured sections, forming the upper part of shallowing-upward cycles (Figure 3). Ooids are generally radially concentric, varying in size from < 0.1 mm to 2 mm, and are often recrystallized to some degree. Bioclasts consist of fragments of trilobites, algae, and echinoderm plates. Individual beds are 2-10 cm thick, with occasional cross laminations. The distribution of ooids and bioclasts is laterally variable along the beds; ooid-dominated beds gradually change to bioclast-dominated beds. Thin (< 3 cm) calcareous shale interbeds are seen between grainstone/packstone layers, particularly at the transition from shale-dominated facies to carbonate-dominated facies in the lower part of the measured sections (Figures 3 and 4). They overlie each other and commonly form an undulated surfaces at the contact (e.g., section BH-7 interval 47-58 m as displayed in Figure 3). This facies is interpreted as having been deposited in shallow subtidal environments close to fair-weather wave base where occasional low-energy conditions occur to allow suspension deposits represented by thin shaly layers.

The cross-bedded oolitic-bioclastic packstone/grainstone facies commonly appears as decimeter- to meter-thick intervals in measured sections (Figures 3 and 4). Thin microbial laminae are common, either along bedding planes of cross stratification (Figure 7a) or as interbeds between grainstone layers (Figure 7b). Packstones are present as interbeds between grainstones layers (e.g., Figure 7c and 7e) or as laterally traceable facies variations of grainstones. The base of cross-bedded grainstone intervals is

commonly erosional (e.g., Figure 7d), with millimeter- to centimeter-scale erosional relief. This facies is interpreted to have been deposited in high- to moderate-energy, shallow subtidal environments above fair-weather wave base (Figure 5); likely environments are within or close to carbonate sand shoals or sand bars.

4.3 Peritidal Microbial Facies Association (FA-3)

The peritidal microbial facies association consists of five facies: (1) flat-wavy microbialites (e.g., Figure 8a-c), (2) oolitic-intraclastic grainstone/rudstone (e.g., Figure 8a and f), (3) fenestral microbialites, (4) thrombolite bioherms/thrombolitic boundstone (e.g., Figure 8d-f), and (5) siliciclastic mudstone and siltstone/silty limestone (e.g., Figure 8a). These facies form 2-15 m thick cycles in the upper part of measured sections (Figure 3) with two arrangements: (1) flat-wavy microbialites capped by mud-cracked siliciclastic mudstone and siltstone, or exposure surfaces with karst breccias, and (2) flat-wavy microbialites that grade upward to thrombolitic bioherms/thrombolitic boundstone and fenestral microbialites. In some intervals, oolitic-intraclastic grainstone/rudstone are present within wavy microbialites boundstone (e.g., Figure 8a).

Flat-wavy microbialites constitute the background lithology in the upper part of measured sections (Figure 3 and 4). Microbialites are composed of interbedded microbial laminae and micritic or lenticular packstone/grainstone laminae. Low-relief domal stromatolites are present in some intervals. Peloids, ooids, and intraclasts are present, but the percentage of these clasts are significantly varied. This facies is interpreted as having been deposited from shallow subtidal to intertidal environments where the substrate was occupied by microbial mats. The presence of coarse-grained particles in micritic and

microbial laminae indicates baffling and binding of sediment particles by microbial mats (Riding, 2000).

Oolitic-intraclastic grainstone/rudstone in this facies association appear as thin (< 5 cm) beds within microbialites, as laterally discontinuous units of a few centimeters to decimeters thick (e.g., Figure 8a), or as localized clusters/blocks in spaces among thrombolite heads (e.g., Figure 8d and f). Thin grainstone beds within microbialites may have been deposited in shallow subtidal environments where carbonate grains (ooids, bioclasts, peloids) from adjacent sand shoals/bars were redistributed by waves and tides. Decimeter-thick grainstone/rudstone units may have deposited in localized carbonate sand bars from shallow subtidal to intertidal microbial mats. Intraclastic grainstone/rudstone among thrombolitic humps is poorly sorted (e.g., Figure 8f), and clasts are sometimes characterized by iron-rich (red) coatings, which suggests reworking and redistribution of desiccated clasts from a subaerial exposure surfaces.

Fenestral microbialites consist of thinly laminated, dark gray, relatively organic-rich layers interbedded with light-colored, irregular, disrupted laminae with fenestral fabric, or of thick layers disrupted by discontinuously bedded, spar-filled fenestrae. Microbial laminae form meter-thick units that commonly cap microbial cycles. Vugs, desiccation cracks, pisolites and karstic breccia are seen in this facies. Fenestral microbial laminae are thought to have formed through the binding of micrite by microbial mats, and to have been preserved as a result of early filling of cavities (formed by organic matter decay) by cement or micrite lithification (Shinn, 1986 cited in Sami and James, 1994). The presence of desiccation cracks, pisolites and karstic breccia is indicative of upper intertidal to supratidal environments (Pratt et al., 1992).

Thrombolite bioherms and thrombolitic boundstone are closely associated. Vertically, laterally continuous thrombolitic boundstone layers grade upward into domal thrombolite bioherms with 30-40 cm relief. Laterally, thrombolite bioherms pinch out within tens of meters and change to thrombolitic boundstone or wavy microbialite. Inter-thrombolite areas are filled with intraclastic/bioclastic grainstone/packstone. Growth forms, morphotypes and lithologic associations within this facies are compatible with low-moderate energy, shallow subtidal to intertidal environments (e.g., Sami and James, 1994).

Siliciclastic mudstone in this facies association is commonly interbedded with thin (1-3 cm thick), laterally discontinuous (or lenticular) siltstone/silty limestone beds and caps some of the peritidal cycles (e.g., Figure 8a). The presence of desiccation cracks in mudstone indicates deposition in upper intertidal to supratidal environments.

4.4 Subaerial Exposure Facies Association (FA-4)

The subaerial exposure facies association includes three facies: karstic breccia, calcrete, and intraclastic rudstone/floatstone. These facies form <10 cm thick, laterally discontinuous layers/lenses that commonly form the tops of cycles. Karstic breccias consist of fragments of microbialites, with dolomitic and silty matrix (e.g., Figure 9a). Clasts are poorly sorted, variable in size from a few millimeters to centimeters, and mostly angular to sub-angular in shape. Breccias were likely formed in paleokarst depressions where carbonates underwent dissolution, fracturing, and brecciation (Mustard and Donaldson, 1990). This facies is interpreted to have formed in supratidal

environments when the carbonate platform was subaerially exposed (Mustard and Donaldson, 1990).

The calcrete facies is characterized by cm-size, light brown to gray, lime-mudstone nodules, coated grains (e.g., aggregates, oncoids, ooids) and rare bioclastic fragments with micritic matrix (e.g., Figure 9b). The calcrete lithofacies is commonly present as 5-15 cm thick layers above the microbialite facies or the grainstone/packstone facies. This facies appears as a laterally discontinuous layers that grade laterally into the intraclastic rudstone/floatstone facies. It is interpreted as the remains of a supratidal paleosols (Mustard and Donaldson, 1990; Bosence et al., 2009).

The intraclastic rudstone/floatstone facies consists of 1–5-cm-sized, dark gray intraclasts in a micritic matrix (e.g., Figure 9c). Intraclasts are sub-angular to sub-rounded and are poorly sorted. This facies forms thin (5-10 cm), lenticular units along bedding surfaces in microbialites, or it fills depressions between thrombolite humps (e.g., FS in Figure 9d). Laterally this facies changes to fenestral microbialites or an exposure surface with karstic breccias. The intraclastic rudstone/floatstone facies is interpreted to have formed in supratidal environments where the intraclasts were produced from desiccation of microbial mats and were reworked by tides and waves during subsequent transgression.

4.5 Evolution of Depositional Environments

Overall, the upper Big Horse Member in measured sections shows a shallowing-upward trend (Fig. 4). The lower part is dominated by deep to shallow subtidal facies that form subtidal cycles. Localized sand bars/dunes were common, and carbonate particles

(ooids, bioclasts, peloids, oncoids) were redistributed by waves and tides to form thin grainstone/packstone beds (Fig. 10a). In comparison with the lower part, the middle part of measured sections is characterized by an increase of microbialites and thrombotic bioherms (Fig. 4 and 10b). The increase of microbialites implies the colonization of microbial mats at least episodically in sedimentary substrates. Isolated thrombotic bioherms formed local obstacles, functionally similar to patch reefs, that differed the energy conditions in shallow subtidal and intertidal environments and led to the formation of laterally variable facies (Fig. 10b). The uppermost part of the Big Horse member is dominated by microbialites, localized thrombotic bioherms and laterally discontinuous grainstone/packstone units characteristic of shallow subtidal to intertidal environments. Subaerial exposure features are common. The dominance of microbial mats in the depositional environments and the limitation of accommodation space resulted in large spatial and temporal facies variations (Fig. 10c).

CHAPTER 5

CYCLES AND CYCLE VARIATIONS

5.1 Cycle Definition and Cycle Types

Meter-scale cycles are the basic building elements of carbonate successions (Tucker and Wright, 1990; Pratt et al., 1992; Goldhammer et al., 1993). In general, carbonate cycles have been defined as “repeated meter-scale sedimentary successions that are made up of different arrangements of deepening- or shallowing-upward facies associations and bounded by different surfaces, such as subaerial exposure or marine flooding surfaces” (Bosence et al., 2009). Based on the relationship between depositional rate and accommodation space, Soreghan and Dickinson (1994) described five generic types of cycles, among which the three common types are: (1) Keep-up cycles, in which the rate of carbonate production outpaces the accommodation creation. Cycles occupy maximum accommodation space but depositional facies may not change significantly through time, resulting in “thickness complete” but “facies incomplete” cycles; (2) Catch-up cycles, in which carbonate production and sedimentation are initially slow, but progressively overtake the accommodation space, resulting in a clear shallowing-upward trend. These type of cycle is “thickness complete” and “facies complete”; and (3) Catch-down cycles, in which, during most of the time, carbonate sedimentation lags behind the accommodation creation, but eventually overtakes it. If the initial deep-water facies are not eliminated, cycles have a condensed lower portion and shallowing-upward upper portion. The resulting cycles are referred to as “foreshortened cycles” with ‘complete’ facies but may or may not have ‘complete’ thickness. If the deep-water facies are

terminated by subaerial exposure and/or erosion, the cycles would be “truncated cycles” formed by forced regression.

Meter-scale cycles are mostly expressed by a shallowing-upward trend, although in some specific depositional settings such as intracratonic basins, deepening-upward cycles have also been documented (e.g., Lukasik and James, 2003). Thus identification of cycles relies on two important criteria: a shallowing-upward trend and the bounding surfaces (exposure or flooding surfaces).

According to these criteria, i.e., shallowing-upward trend and bounding surfaces, three types of cycles have been identified from the upper Big Horse Member of the Orr Formation (Figure 11). These cycles include (1) microbialite-rich peritidal cycles, (2) thrombolite-capped cycles, and (3) packstone/grainstone-capped subtidal cycles.

5.1.1 Microbialite-rich Peritidal Cycles

Microbialite-rich peritidal cycles are 4-20 m thick and composed of component facies of the peritidal microbial facies association (Figures 3 and 11). Cycles commonly start with flat-wavy microbialite facies that grade upward to fenestral microbialite facies and are capped by a karstic surface or an erosional surface with lag deposits represented by intraclastic rudstone/floatstone. Siliciclastic mudstone/siltstone with desiccation cracks caps the cycle and forms a keep-up cycle (e.g., Figure 8a). In some cases, mixed shale and limestone, and oolitic/bioclastic packstone/grainstone beds appear at the base or middle of the cycle, forming ‘catch-up’ cycles.

The number of component facies in individual cycles varies from 2 to 5 facies. Their common combinations include:

- (1) Flat-wavy microbialite → exposure facies (karstic breccia, calcrete, or siliciclastic mudstone/siltstone) or fenestral microbialites. Examples (Figure 3) include the upper part of BH2 (106-112 m), BH3 (45.5-59 m), BH4 (95-103 m), BH6 (84-93 m), and BH7 (80-93 m).
- (2) Mixed shale and limestone (packstone and wackestone) → flat-wavy microbialite → fenestral microbialite → oncolid/intraclastic grainstone/rudstone. Examples (Figure 3) include BH7 (47.5-64 m), BH1 (0-8 m, 19-27.5 m, and 27.5-38 m).
- (3) Mixed shale and limestone → cross-bedded oolitic-bioclastic packstone/grainstone mixture with microbial mats → flat-wavy microbialites → exposure surface. Examples (Figure 3) include BH7 (27-47.5 m) and BH4 (82-103 m).
- (4) Cross-bedded oolitic-bioclastic packstone/grainstone associated with microbial → flat-wavy microbialites → thin packstone-grainstone → exposure surface. Examples (Figure 3) include BH4 (69-79 m) and BH7 (67.5-80 m).

Critical for the identification of these cycles are cycle boundaries, which are expressed as karstic/erosional surfaces or other evidence for subaerial exposure features (i.e., desiccation cracks, breccia). In some cases, these cycles contain centimeter-scale facies alternations that may be sub-meter-scale cycles (e.g., the interval from BH4 and BH5 as shown in Figures 15). The sub-meter-scale cycles were possibly formed during the late stage of a meter-scale cycle, during which frequent exposure of the intertidal environment and siliciclastic input from a supertidal environment formed multiple exposure surfaces above thin silty-muddy limestone (Figure 16).

5.1.2 Thrombolite-capped Cycles

In the studied sections, eleven thrombolite-capped cycles can be distinguished, and they have a wide range of thickness varying from 2 to 36 m. In the lower and middle part of the measured sections (Figure 3), thrombolite-capped cycles commonly start with deep-subtidal facies (calcareous shale and siltstone-silty limestone or mixed shale and limestone) and shallow subtidal facies (cross-bedded oolitic-bioclastic pack-grainstone). These grade upward to thrombolitic boundstone and thrombolite with synoptic relief, and are capped by thin layers of oolitic-intraclastic packstone/grainstone. In the upper part of measured sections, thrombolite-capped cycles start with flat-wavy microbialites or interbedded packstone and wackestone, followed by thrombolites and intraclastic rudstone/floatstone among thrombolite humps. Reworking of desiccated clasts from subaerial exposure surfaces during subsequent transgression likely formed intraclastic rudstone/floatstone.

In the lower part of the measured sections (e.g., BH4, BH5, and BH6; Figures 3 and 17), thrombolite-capped cycles laterally merge into other thick and massive thrombolite cycles or interfinger with type-3 cycles (grainstone/packstone-capped cycles). In the middle and upper part of the sections, thrombolite-capped cycles grade laterally into microbial-rich peritidal cycles (e.g., the uppermost cycle in BH2 and BH4; the middle part of BH6 and BH7; Figures 3 and 17). Lack of lateral continuity of this type of cycle is related to the localized nature of thrombolite bioherms, which are present as localized or patchy forms.

5.1.3 Grainstone/packstone-capped Subtidal Cycles

Ten grainstone/packstone-capped subtidal cycles varying in thickness from 8 to 35 m are documented from measured sections (Figures 3 and 11). These cycles commonly start with deep subtidal facies (calcareous shale and silty limestone or mixed shale and limestone) and end with cross-bedded oolitic-bioclastic packstone/grainstone. Cycles are bounded by flooding surfaces expressed by an abrupt facies change from pack-grainstone to calcareous shale at the top of each cycle. These cycles are present only in the lower part of measured sections, except in section BH3. The grainstone/packstone facies in section BH3 include abundant microbial laminae at the bedding planes of cross beds, implying relatively higher energy environments compared with other sections (Figure 7a and b).

Subtidal cycles are mostly present in the lower part of measured sections (Figure 3). The lower part of individual cycles was likely formed during times of low production and sufficient accommodation space, while the top of the cycles represents a fast shallowing and reduction in accommodation in the depositional site. These cycles are similar to the “catch-down” cycles described by Soreghan and Dickinson (1994).

5.2 Temporal and Spatial Variation of Cycles

The most important feature of cycles from the Big Horse Member is their temporal and spatial variations. Vertically in each section, cycles vary in thickness from 3 to 36 meters (Figure 3). If the cycles are not laterally traced, they appear as cyclic, as has been documented in numerous publications. However, comparing the cycles among sections indicates that the cycle numbers in equivalent intervals (constrained by traceable

surfaces) differ (Figures 3 and 4). Examples showing lateral variation of cycles in the upper part of the studied interval are provided in Figures 11-15. For example, among three microbialite-rich peritidal cycles in the upper part of section BH4, one of them disappears within 200 m towards section BH5 and section BH3 (Figures 15). Similarly, two of the three cycles in the middle part of section BH4 disappear toward section BH3, and one of them pinches out toward section BH5 (Figure 15). Similarly, one of the three cycles identified between S2 and S3 in section BH6 disappears in BH7 (Figures 12 and 13), which is only 250 meters away. Variations in cycle thickness are also obvious in the lower part of the Big Horse Member (Figure 3), but lateral tracing of cycles in this part is more difficult because of less well-exposed outcrops compared with the upper part.

Carbonate cycles have been proposed to have hierarchies and those at the same hierarchy may record approximately the same amount of time (i.e., Koerschner and Read, 1989; Goldhammer et al., 1993). Although the upper Big Horse Member shows an overall shallowing-upward trend (Figure 4), the cycles of varying thickness do not show an obvious hierarchy in which thinner cycles (high-frequency cycles) are supposed to stack together to form the thick cycles (low-frequency cycles). The amount of time represented by these cycles is difficult to evaluate, but their vertical stacking pattern (Figure 3) suggests that meter-scale cycles in the same section may have formed over significantly variable interval of depositional time.

CHAPTER 6

DISCUSSIONS

6.1 Formation of Meter-scale Cycles

Shallowing-upward peritidal and subtidal cycles have been interpreted as laterally continuous units that can be correlated for hundreds of kilometers (e.g., Grotzinger, 1986; Osleger and Read, 1991; Goldhammer et al., 1993). However, only occasionally have facies and cycles been traced to prove their later continuity (e.g., Pratt and James, 1986; Adams and Grotzinger, 1996; Jiang et al., 2003). The large temporal and spatial variations of meter-scale cycles of the Big Horse Member provide a unique example for understanding the lateral variation of cycles in sufficiently well exposed outcrops.

In general, regionally consistent cycles have been interpreted as having formed by astronomically driven sea-level changes (e.g. Koerschner and Read, 1989; Goldhammer et al., 1990, 1993). The lateral variability of cycles over a distance of hundreds of meters within the Big Horse Member is unlikely to have originated from glacioeustatic-controlled cycles as previously discussed by Osleger and Read (1991). Instead, the lateral variation of cycles is better interpreted as modified versions of the tidal-flat island model (Pratt and James, 1986; Sami and James, 1994). Local variation in carbonate production and siliciclastic input in microbially colonized, shallow subtidal to intertidal environments, may lead to the formation of multiple exposure surfaces (thus multiple cycles) in areas close to the clastic source (Figure 16). Similarly, the uneven distribution of carbonate sand dunes/bars in subtidal-dominated environments may result in lateral variability of subtidal cycles, while migration of carbonate sand dunes/bars and thrombolite bioherms may form laterally variable peritidal cycles (Figure 17).

The cycle-formation mechanisms have been slightly different within the three stratigraphic intervals divided by laterally correlatable exposure surfaces (S1, S2, S3 in Figures 3 and 4). If each exposure surface represents zero accommodation space, an episode of tectonic subsidence is necessary to create the accommodation required for the deposition of subsequent cycles (Figure 17). During the deposition of the lower part of measured sections, deep subtidal environments dominated. Migration of locally developed, shallow subtidal carbonate sand shoals/bars formed the grainstone/packstone-capped subtidal cycles (Figure 17a). At the end of this interval, carbonate sand shoals extended and covered the entire study area, with local thrombolite bioherms developed at the top. The end of this interval is represented by a karstic surface (S3), indicating the filling of available accommodation space. The subsequent creation of accommodation space was most likely caused by an episode of tectonic subsidence. After an episode of tectonic subsidence, the middle part of the studied sections experienced initial transgression and deepening, but soon changed to shallow-subtidal-dominated environments (Figure 17b). Migration of carbonate sand shoals and the local development of thrombolite bioherms created meter-scale cycles that are laterally discontinuous. Creation of the accommodation space needed for the deposition of the upper part of the measured sections requires another episode of tectonic subsidence, shortly after the development of surface S2. The background depositional environments representative by these intervals were microbially colonized peritidal environments, within which local development of carbonate sand bars and thrombolite bioherms formed the laterally discontinued cycles (Figure 17c).

The greatest challenge to the autocyclic interpretation presented above is the repetitive generation of accommodation space required for subsequent cycle formation. For example, after a certain time interval, the entire Little Horse Canyon area would have been exposed and no accommodation space could be available for deposition. In the allocyclic model, a glacio-eustatic sea-level rise creates the accommodation space required for the deposition of subsequent cycles. In the autocyclic model, tectonic subsidence is left as the option for the creation of accommodation space (e.g., Lukasik and James, 2003; Spence and Tucker, 2007; Bosence et al., 2009). However, tectonic subsidence may not be as regular as astronomically driven sea-level changes that show predictable periodicity.

The temporal variations in cycle number and thickness (and potentially time) of the Big Horse Member provide clues concerning the expected outcome of tectonically created accommodation space. Episodic tectonic subsidence, likely controlled by local faulting overprinted over thermal subsidence of the Furongian carbonate platform, may have created accommodation space at irregular time intervals. Depositional occupancy of available accommodation space resulted in the temporal variation in cycle thickness. Therefore, cycles identified from the Big Horse Member do not represent the same amount of time.

6.2 Implications for Cyclostratigraphy in Greenhouse Carbonate Platforms

The temporal and spatial variability of cycles from the Big Horse Member provide insights into the cyclostratigraphic concept in greenhouse carbonate platforms. In general, if cycles are measured in only one section, they show repetitive patterns as has been

documented in numerous publications. However, when traced laterally, the cycle numbers and thicknesses vary. This phenomenon suggests that individual cycles do not represent an equal amount of depositional time, and the cycle hierarchy system cannot be organized using cycle thickness.

In cyclostratigraphic studies, it has been proposed that, using the cycle stacking patterns and their hierarchy (established by their net thickness changes), cycles can be correlated regionally or even globally (e.g., Koerschner and Read, 1989; Goldhammer et al., 1990; Osleger and Read, 1991). The graphic expression of this concept, namely the Fisher plot (Fischer, 1964), has been used to track the net accommodation change in carbonate successions (e.g. Osleger and Read, 1991; Bosence et al., 2009). The temporal variation of cycles from the Big Horse Member call attention to this practice because individual cycles may not represent equal depositional time, and the creation of accommodation space in the platform may be chronologically irregular. Thus, cyclostratigraphic and sequence stratigraphic studies in greenhouse carbonate platforms similar to the Furongian carbonate platform require identification and correlation of major physical surfaces of regional significance calibrated by geochronological and biostratigraphic data.

CHAPTER 7

CONCLUSIONS

A detailed sedimentological study of the Big Horse Member (Furongian) in closely spaced (200-1100 meter away) and traceable sections of the Little Horse Canyon, western Utah, reveals significant spatial and temporal variations of meter-scale carbonate cycles. Component facies of meter-scale cycles pinch out over a distance of hundreds of meters, and cycle boundaries disappear in conformable facies associations.

Such meter-scale cycle variations are better interpreted as having formed by autogenic processes controlled by tidal island aggradation combined with tectonic and thermal subsidence. Vertical changes in cycle thickness may record episodic, subsidence creation of accommodation space that does not require equal periodicity. The lateral variation of cycles can be explained by the modified tidal-island model in which lateral facies migration controlled the cycle number and cycle thickness in particular depositional environments. Cycles from the Big Horse Member provide a unique example for understanding the lateral variation of cycles in sufficiently well-exposed outcrops and lend insights into cyclostratigraphic study in climatically similar carbonate platforms.

Table 1. Summary of facies and facies associations of the Big Horse Member

Lithofacies	Constituents	Bedding and structures	Interpretation
DEEP SUBTIDAL FACIES ASSOCIATION (FA-1)			
Calcareous shale and siltstone (silty limestone)	Grey to light grey color; siltstone and silty limestone layers 2-5 cm thick; 20-25% silty grains in limestone layers; thin lime mudstone interbeds (millimeters); chert nodules, mud drapes, and burrows are common	Laterally continuous, millimeter- thick parallel lamination; small-scale wavy cross-lamination in silty layers; thickness of silty limestone layers varies from 2 to 5 cm	Deep subtidal below fair weather wave base
Mixed shale and limestone	Unevenly interbedded calcareous shale/siltstone and lime mudstone-wackestone; rare fine-grained peloidal grainstone	Laterally continuous, millimeter- thick parallel lamination; rare wavy cross-lamination with minor erosional surfaces in grainstone layers; shale-limestone alternation	Deep subtidal, occasionally shallowing to wave base
SHALLOW SUBTIDAL FACIES ASSOCIATION (FA-2)			
Oolitic-oncolitic packstone	Micritic oncoids, 2-10 mm in diameter; 10-50% grain content; rounded-spherical; ooids < 0.1 to 2mm in size, spherical and concentric; alternating ooid-rich and oncoid-rich layers; poor sorting in oncoidal layers but well-sorted in oolitic layers; sparry calcite matrix	Tabular to lenticular units; beds laterally discontinuous; wavy bedding and ripple cross laminations	Shallow subtidal close to or above fair-weather wave base
Oolitic-bioclastic packstone/grainstone	Radial concentric ooids < 0.1- 2 mm in diameter; partially micritized and dolomitized; bioclastic fragments of trilobites, algae, echinoids, and crinoids; sparry calcite cements with subordinate micrite matrix; thin calcareous shale interbeds	Cross laminations; laterally discontinuous beds	Shallow subtidal above fair- weather wave base; occasional low-energy environments (shale)
Cross-bedded oolitic-bioclastic packstone/ grainstone	70-90% grains; mixture of radial and broken ooids/pellets, microbial clasts, trilobites, phylloid algae, echinoids, crinoids	Abundant large-scale cross-bedding and small-scale cross-lamination	Shallow subtidal carbonate sand shoal or sand bars

PERITIDAL MICROBIAL FACIES ASSOCIATION (FA-3)

Wavy microbialites	Thin microbial laminae interbedded with micritic or lenticular grainstone laminae; laterally-linked, low-relief stromatolites; peloids, stromaclasts, ooids, and intraclasts	Millimeter-thick, interbedded, undulating, micritic laminae; clasts preserved in small ripples or as fill between stromatolite humps; wave ripples and flaser bedding	Shallow subtidal to intertidal
Oncoid/intraclastic grainstone/rudstone	Intraclasts typically 0.5-2 cm (up to 5 cm) with surficial coatings; matrix of lime mudstone and fine-grained peloids, ooids and bioclasts	Tabular to lenticular, discontinuous beds; commonly associated with microbial, thrombolitic boundstone and thin oolitic grainstone layers; small-scale cross-lamination and ripples	Shallow subtidal to intertidal
Fenestral microbialite	Grey laminae interbedded with light-colored, irregular, disrupted beds of fenestral fabric; or thick microbial boundstone layers disrupted by small, discontinuously bedded, spar-filled fenestrae	Poor to moderate lateral continuity; low-relief domal stromatolites/thrombolites; fenestral structures, vugs, desiccation cracks and brecciation	Upper intertidal to supratidal
Thrombolite bioherms / Thrombolitic boundstone	Laterally continuous thrombolitic boundstone in the lower part grading upward to domal thrombolite bioherms 30-40 cm high; intraclastic/bioclastic grainstone/packstone filling spaces between thrombolitic bioherms	Laterally discontinuous; isolated or laterally linked bioherms forming thrombolitic complex	Shallow subtidal to intertidal
Siliciclastic mudstone and siltstone/silty limestone	Yellowish to grey siliciclastic mudstone interbedded with 1-3 cm thick, lenticular siltstone and silty limestone.	Laterally discontinuous siltstone/silty limestone beds; desiccation cracks	Intertidal to supratidal

SUBAERIAL EXPOSURE FEATURES (FA-4)

Karstic breccia	Mostly clasts similar to host; poorly sorted or unsorted, sub-angular to angular clasts of varying sizes from < 1cm to 3 m; sandy, silty, and micritic matrix	Thin beds or lenses of varying thickness (5-50 cm thick) along exposure surfaces; vadoose cements around breccias	Surface certification products; caustic depression fills
Accrete	Cm-size micrite nodules, reddish silty limestone layers, coated grains and intraclasts	Laterally discontinuous, 5-10 cm thick	Sub-aerial exposure

Intraclastic rudstone/floatstone	Sub angular intraclasts (1 - 10 cm long), muddy limestone matrix	Thin (5 - 10 cm), lenticular units along bedding or infill between thrombolite humps; laterally change into fenestral microbialites or exposure surface with breccias	Reworked clasts from sub-aerial exposure surface
-------------------------------------	---	--	--

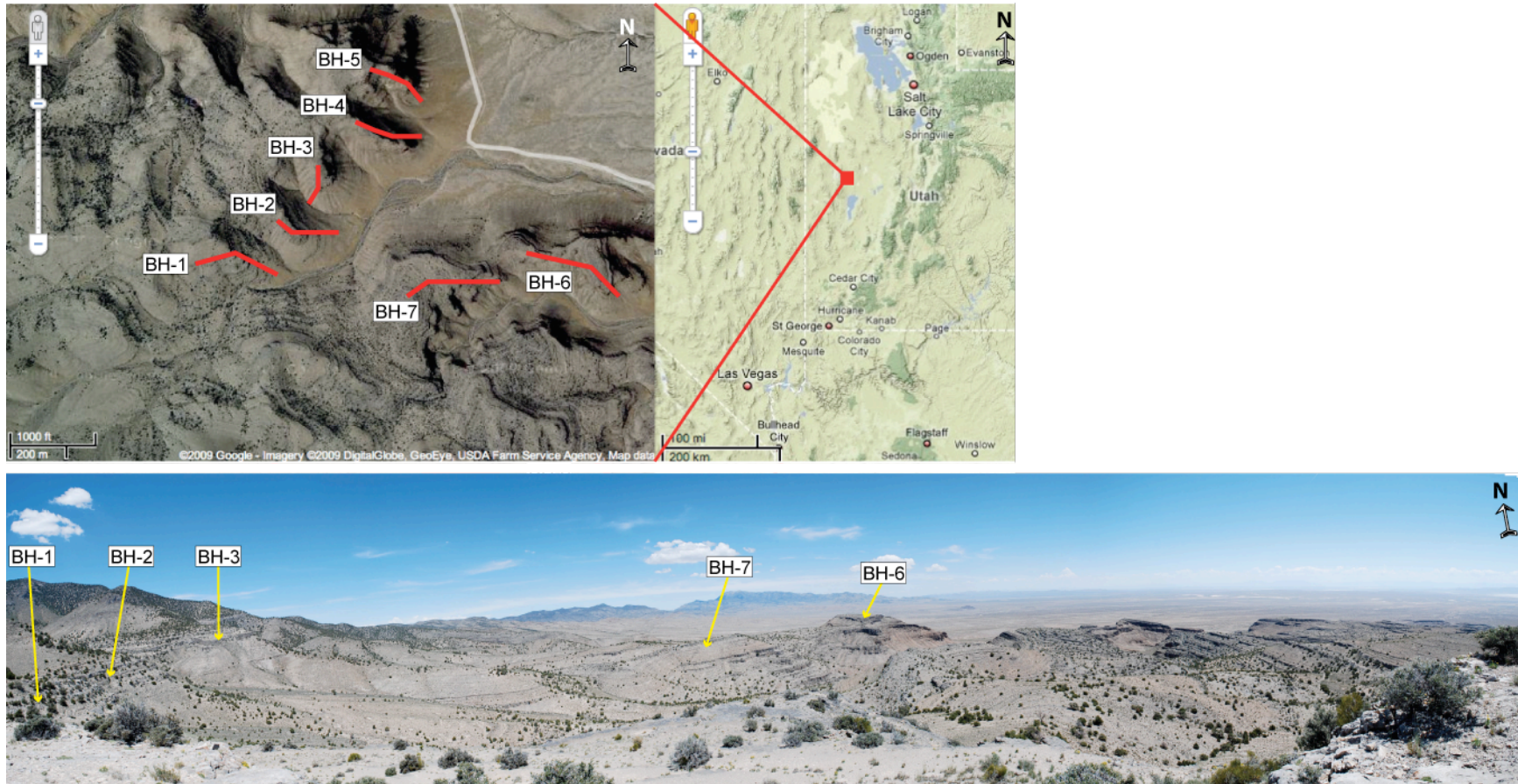


Figure 1. **(a)** A google earth image and map showing the location of study area in the Little Horse Canyon, western Utah. The location is at $N 39^{\circ} 12.412'$, $W 113^{\circ} 18.450'$. **(b)** The outcrop consists of the Big Horse Member of the Orr Formation, which was deposited during early Furongian time (see Figure 2). The excellent exposure in this area allows for a detailed sedimentological study in closely spaced sections (BH1 – BH7) and for lateral tracing of key surfaces, cycles, and facies.

AGE	FORMATION	STAGES	BIOMERE	TRILOBITE ZONES
Furongian (Late Cambrian)	Orr Formation	Steptoean	Pteropcephaliid	<i>Taenicephalus</i>
				<i>Elvinia</i>
				<i>Dunderbergia</i>
				<i>Prehousia</i>
				<i>Dicanthopyge</i>
				<i>Aphelapis</i>
Cambrian Series 3 (Middle Cambrian)	Weeks Limestone (366 m)	Marjuman	Marjumiid	<i>Crepicephalus</i>
				<i>Cedaria</i>
				<i>Bolaspidella</i>
Marjum Formation (415-430 m)				<i>Ehmaniella</i>

82 m
 Studied interval

Figure 2. Stratigraphic column of the Orr Formation in the House Range, western Utah. The studied interval is stratigraphically located in the upper Big Horse Member of the Orr Formation (uppermost *Crepicephalus* part) (modified from Saltzman et al., 1998; Kellogg 1963; Palmer, 1971; Rees and Robison, 1989).

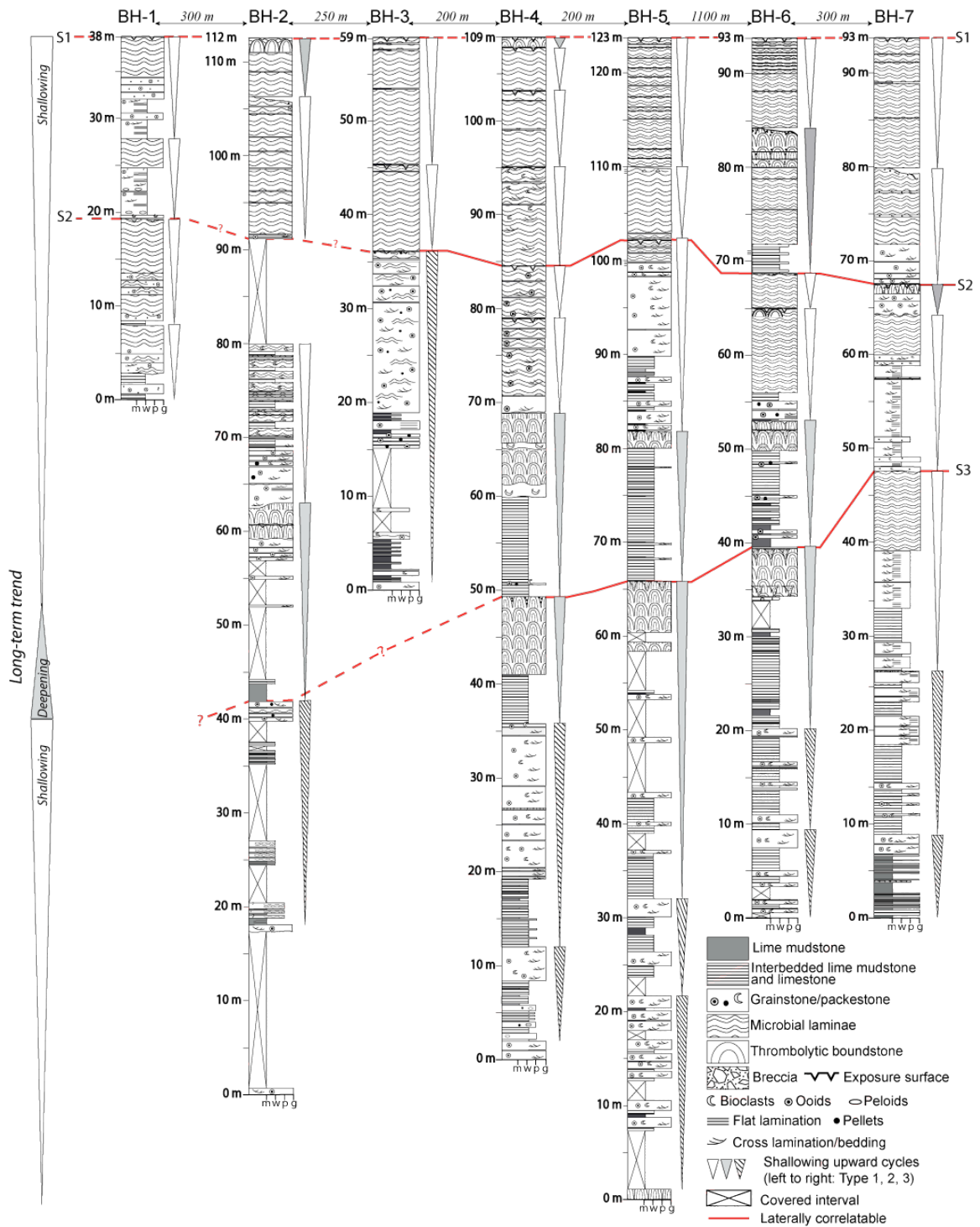
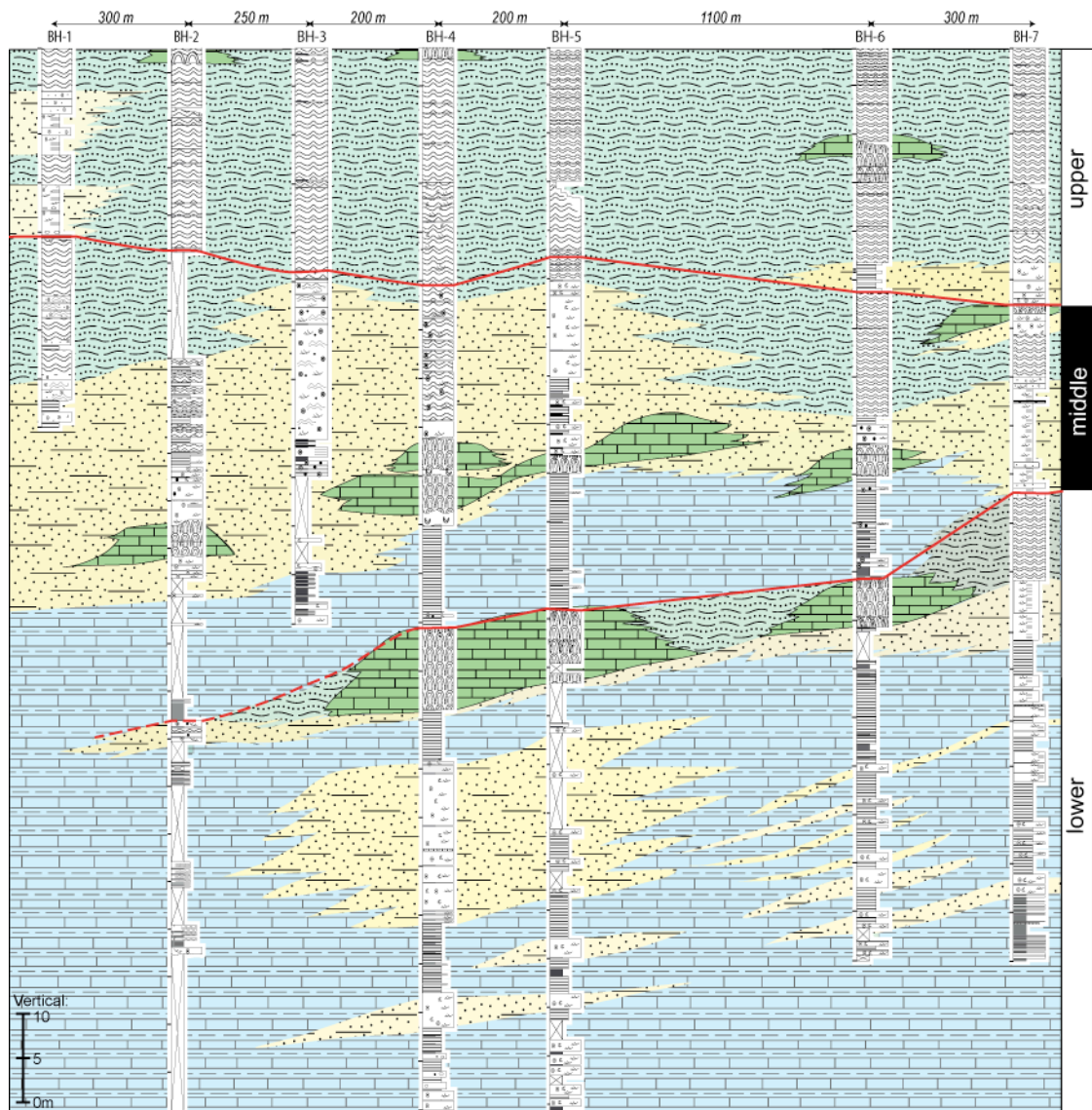


Figure 3. Stratigraphic column from seven sections of the upper Big Horse Member in the Little Horse Canyon, western Utah. Meter-scale cycles show temporal and spatial variations among sections. Surface S1, S2, and S3 represent exposure surfaces traceable (solid line) or correlatable (dashed line) between sections.



Lateral correlation:

- | | |
|--|---|
|  Deep subtidal facies association (FA-1) |  Peritidal microbial facies association (FA-3) |
|  Shallow subtidal facies association (FA-2) |  Thrombolytic bioherm (part of FA-3) |

Figure 4. Lateral facies variations of the studied interval within the Big Horse Member. S1, S2, and S3 are used as reference horizons to track the facies variations among sections and to divide the interval into upper, middle, and lower parts.

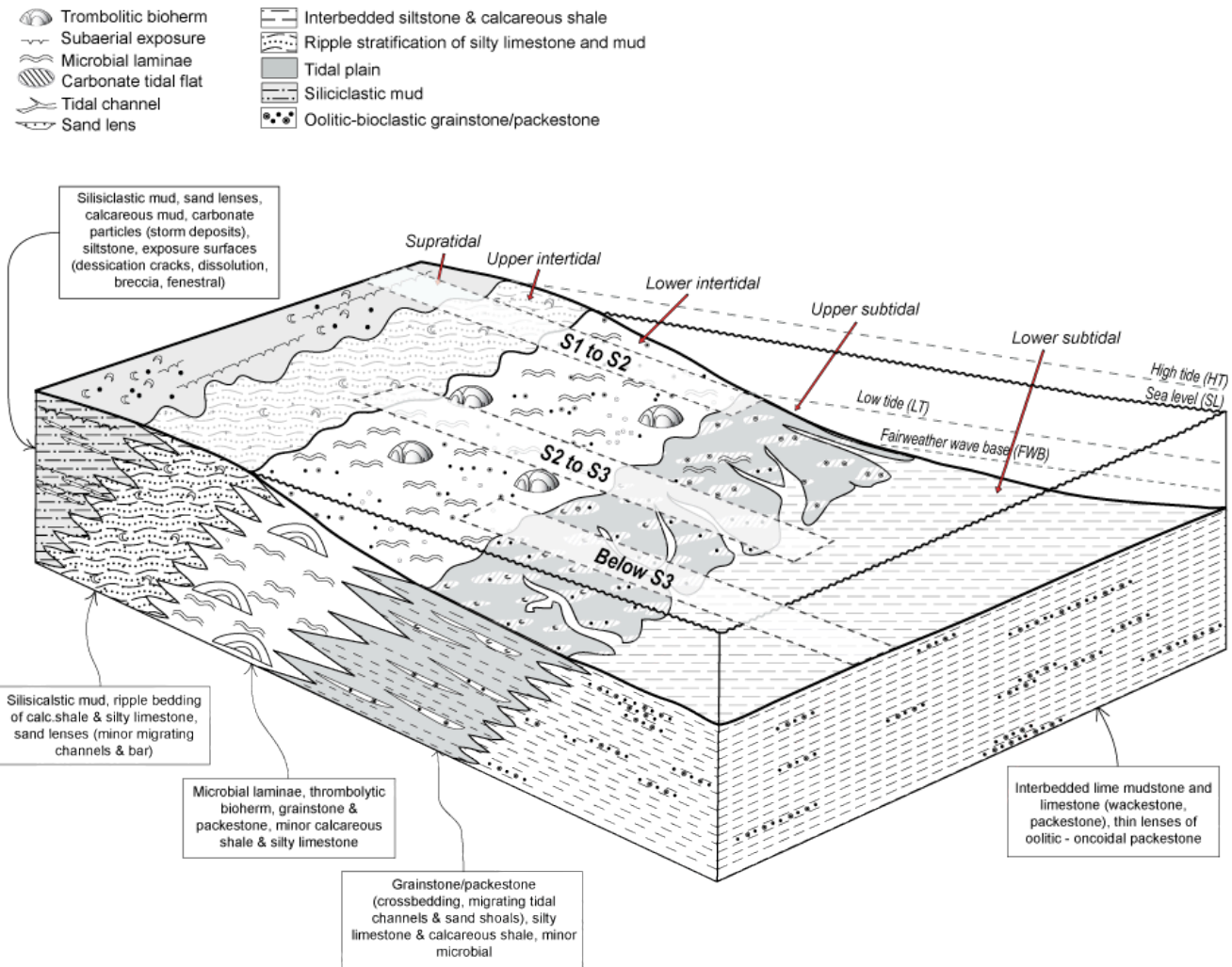


Figure 5. Generalized depositional model and the distribution of lithofacies and facies associations in the Big Horse Member.

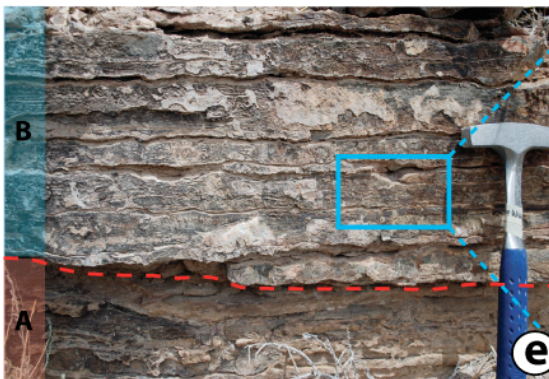
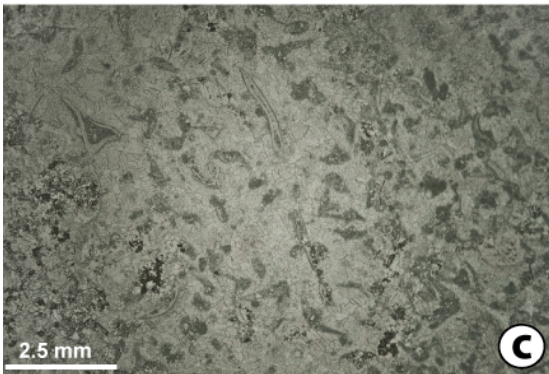
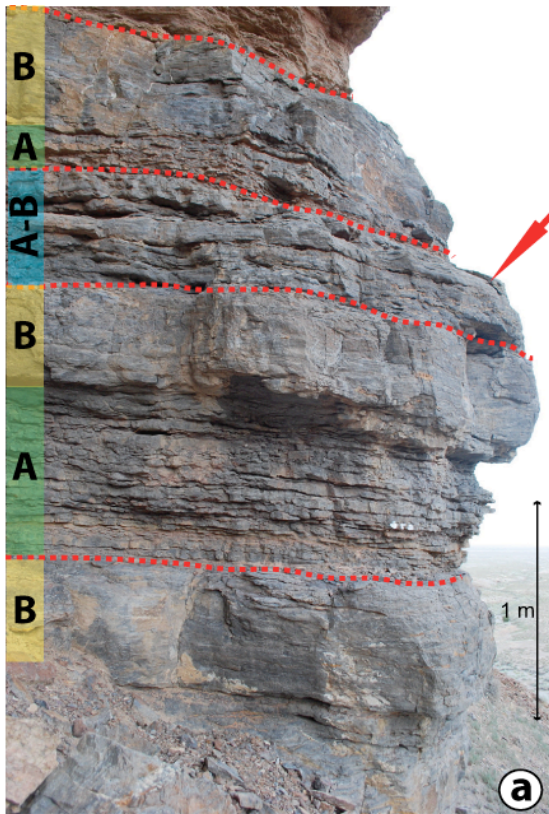


Figure 6. Field and petrographic photos of deep and shallow subtidal facies associations. **(a)** Interbedded calcareous shale and silty limestone (A) and packstone (B) (taken from BH-4 interval 2-5.2 m). Parallel-laminated calcareous shale and lime mudstone layers in (A) show nodular structures due to differential compaction, in which limestone layers vary in thickness from 2 to 5 cm. The overlying peloidal and oolitic packstone unit (B) is commonly 40-50 cm thick, with minor lime mudstone lenses. Interbedded calcareous shale and lime mudstone (A) are interpreted as having deposited from low-energy, deep subtidal environments below fair-weather wave base (FWWB). **(b)** Detailed view of the packstone unit showing laterally discontinuous lime mudstone lenses. **(c)** Bioclastic packstone equivalent to (B) from BH-3 section (from BH-3 section at 8 m level). **(d)** Laminated calcareous shale and lime mudstone (deep subtidal facies) from BH-4 section (interval 6-9 m). **(e)** Interbedded calcareous shale and silty limestone (A) and bioclastic packstone (B) from BH3 section at 5 m. **(f)** Enlarged view of the bioclastic packstone interval showing cross laminations, minor siltstone beds/lenses, and bioturbation. Hammer for scale is 32.5 cm long.

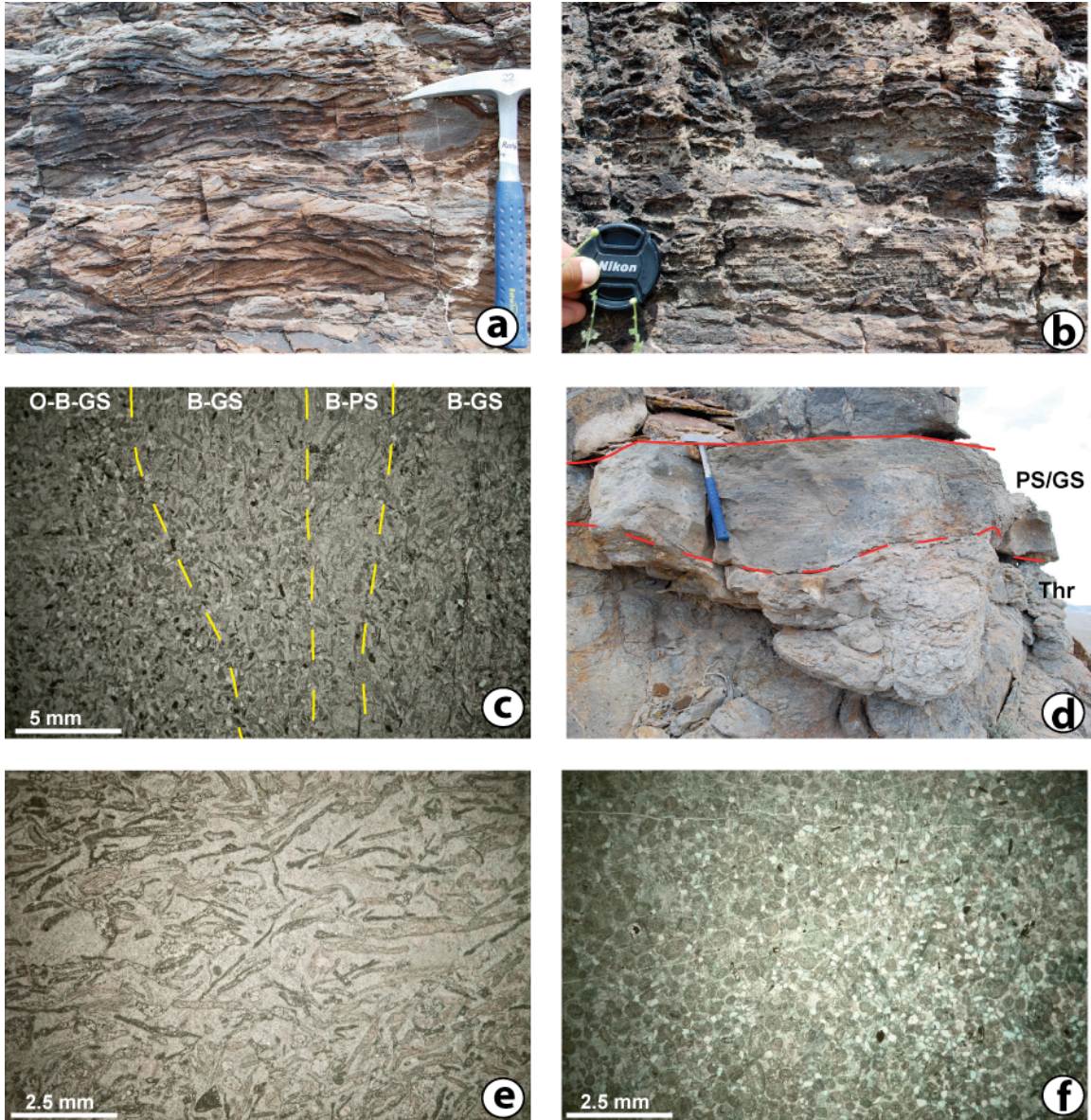


Figure 7. Field and petrographic photos of the shallow subtidal facies association. **(a)** Bioclastic and oolitic grainstone showing cross stratification (from section BH-3, interval 19 m). Microbial laminae along bedding planes of cross stratification imply the importance of microbial processes in formation and preservation of cross beds. Hammer for scale is 32.5 cm long. **(b)** Interbedded microbial laminae and cross-stratified grainstone/packstone. Microbial laminae are laterally discontinuous and pinch out towards thick grainstone/packstone beds. **(c)** Petrographic view of the alternating oolitic-bioclastic grainstone (O-B-GS), bioclastic grainstone (B-GS), and bioclastic packstone (B-PS). Plane polarized light. From section BH-3 at 23.5 m. **(d)** Relationship between bioclastic-intraclastic packstone/grainstone and thrombolitic bioherm. The karstic surface (dashed line) between the grainstone/packstone layer and its underlying bioherm marks the top of a thrombolite-capped cycle. Hammer for scale is 32.5 cm long. **(e)** Thin section view of the bioclastic packstone from section BH-4 at 1 m. Bioclasts include fragment of

ostracods, crinoids, echinoderm plates, and algae. Cross-polarized light. **(f)** Well-sorted, oolitic grainstone from section BH-3 at 0.1 m. Cross-polarized light.

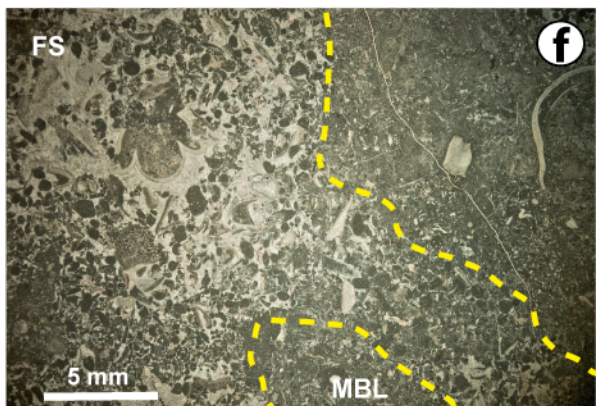
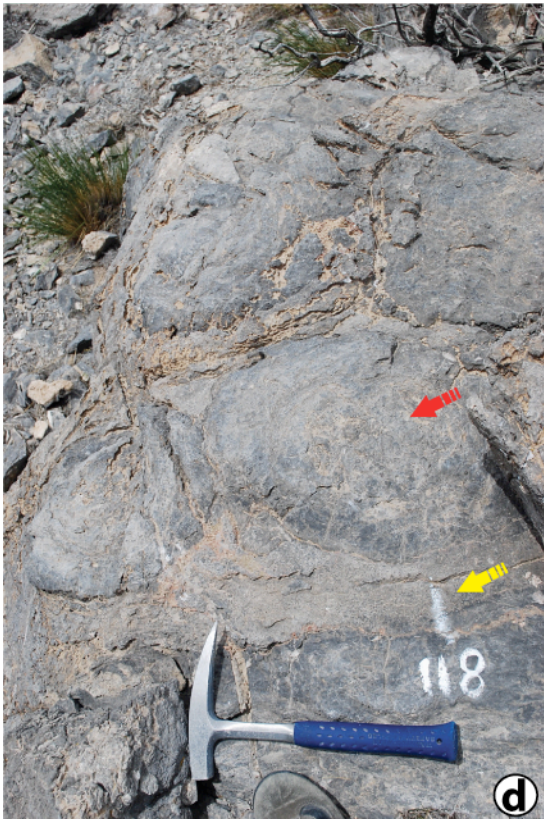
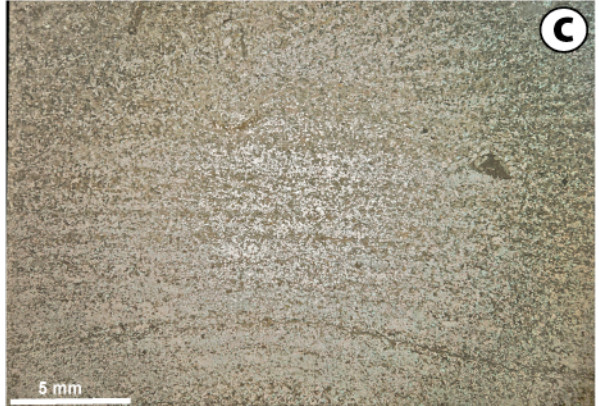
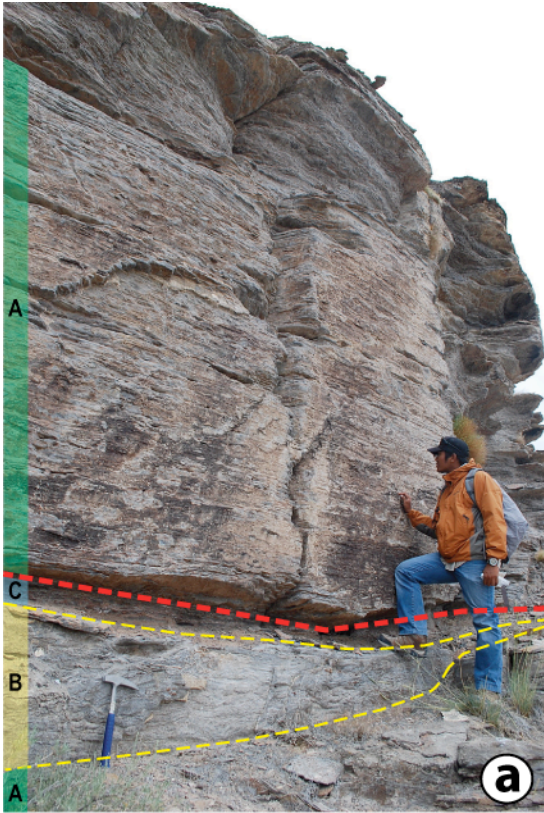


Figure 8. Field and petrographic photos of the peritidal microbial facies association. **(a)** Field photo showing the change from flat and wavy microbialites (A) to oolitic grainstone (B) and thin siliciclastic mudstone and silty limestone (C). A to C marks a shallowing-upward cycle. The photo is taken from section BH-7 at interval 74-77.5 m. Hammer for scale is 32.5 cm long. **(b)** Flat microbial laminae interbedded with thin calcareous shale and silty limestone at the uppermost 2 m of section BH5 (Figure 3). **(c)** Photomicrograph of microbial laminae showing the binding of mud and silt by microbial mats. Plane polarized light. **(d)** Plane view of thrombolitic bioherms (red arrow). Thrombolite humps have sizes from 30-40 cm in diameter. Inter-thrombolites are commonly filled with intraclastic grainstone/packstone (yellow arrow). **(e)** Gradual change of wavy microbialites into thrombolitic bioherm. Laterally, thrombolitic bioherms pinch out and change to microbialites. Thin grainstone/packstone layers and calcareous shale/siltstone lenses are seen in microbialite-dominated intervals. **(f)** Microscopic view of intraclastic/bioclastic floatstone (FS) as the lag deposit in between microbialites (MBL).

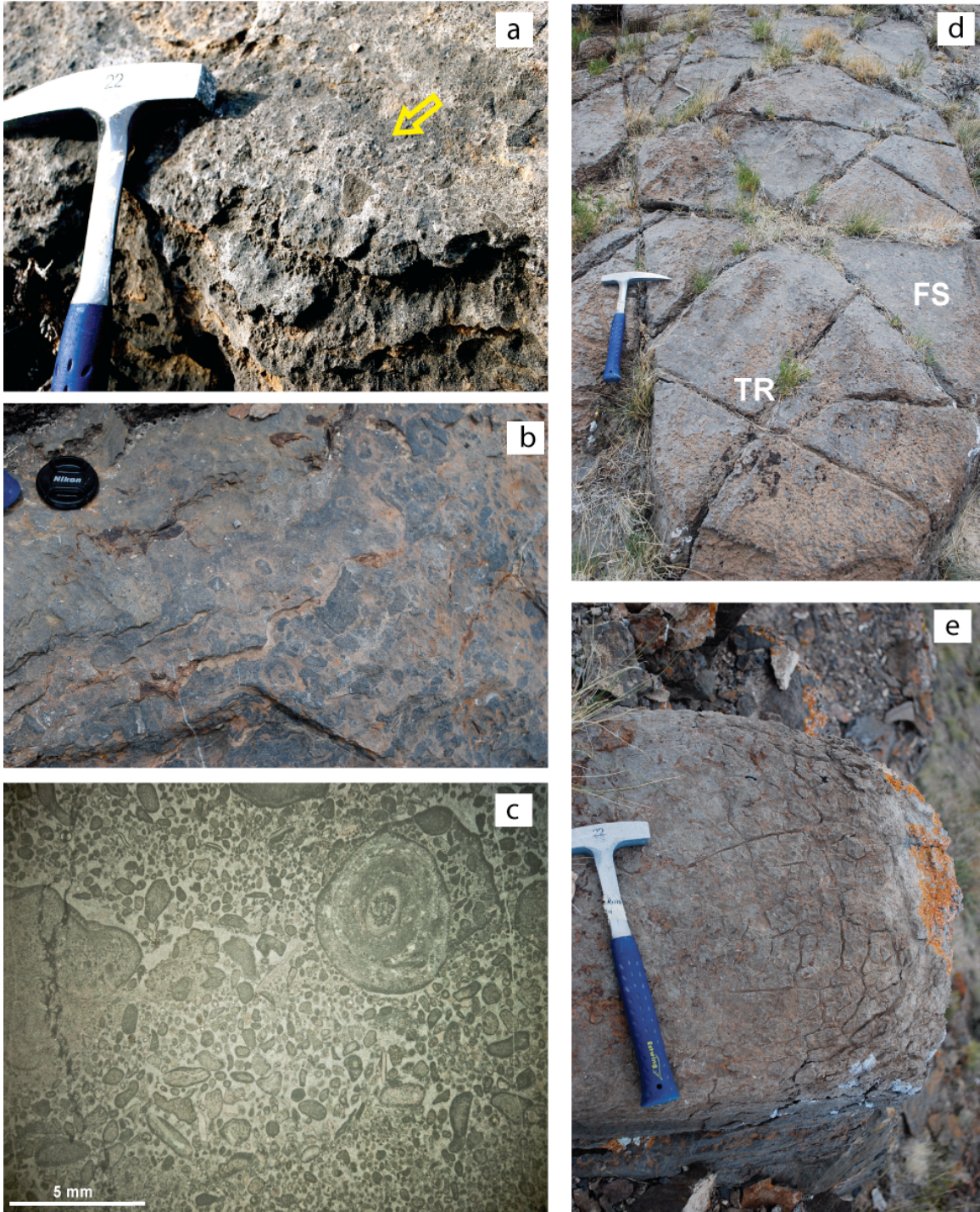


Figure 9. Subaerial exposure features. **(a)** Lithoclasts (yellow arrow) with silty dolostone matrix (karst breccia) along a karstic surface, occurs at 38 m in section BH1. **(b)** Cemented coated grains commonly appear as calcrete facies on an exposure surface. Lens cap for scale is 76 mm in diameter. **(c)** Intraclastic rudstone/floatstone commonly appear discontinuously along an exposure surface and consist of carbonate aggregates, oncoids, pellets, and ooids. Plane polarized light. **(d)** Thrombolite humps (TR) and rudstone/floatstone (FS) filling the spaces among thrombolite humps (FS, i.e., aggregates, and rudstone).

bioclasts, intraclasts, siliciclastic mud, pellets forming rudstone/floatstone). (e)
Desiccation cracks on the top of thrombolite humps.

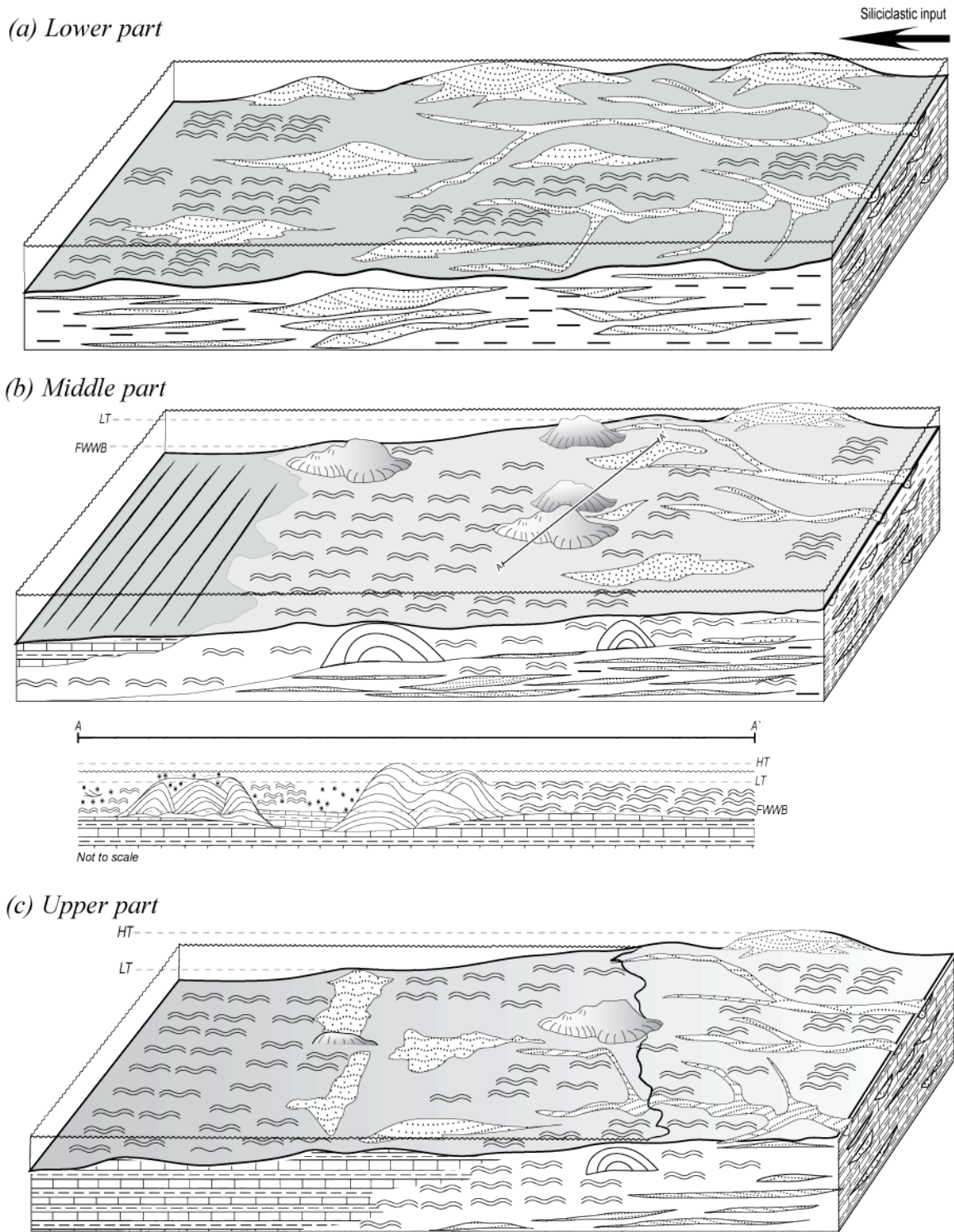


Figure 10. Schematic temporal evolution of depositional environments. In general, the upper Big Horse Member shows a shallowing-upward trend (Fig. 4). (a) The lower part of measured sections is dominated by deep to shallow subtidal facies that form subtidal cycles. Localized sand bars/dunes were common and carbonate particles (oids, bioclasts, peloids, oncoids) were redistributed by waves and tides to form thin grainstone/packstone

beds; (b) In comparison with the lower part, the middle part of measured sections is characterized by an increase of microbialites and thrombotic bioherms. The increase of microbialites implies the colonization of microbial mats at least episodically. Isolated thrombotic bioherms formed local obstacles functionally similar to patched reefs that differentiated the energy conditions in shallow subtidal and intertidal environments and led to formation of laterally variable facies; (c) The upper part of measured sections is dominated by microbialites, localized thrombotic bioherms and laterally discontinuous grainstone/packstone units. Subaerial exposure features are common. The dominance of microbial mats in the depositional environment and limitation of accommodation space resulted in large spatial and temporal facies variations. Abbreviations are the same as on Figure 5.

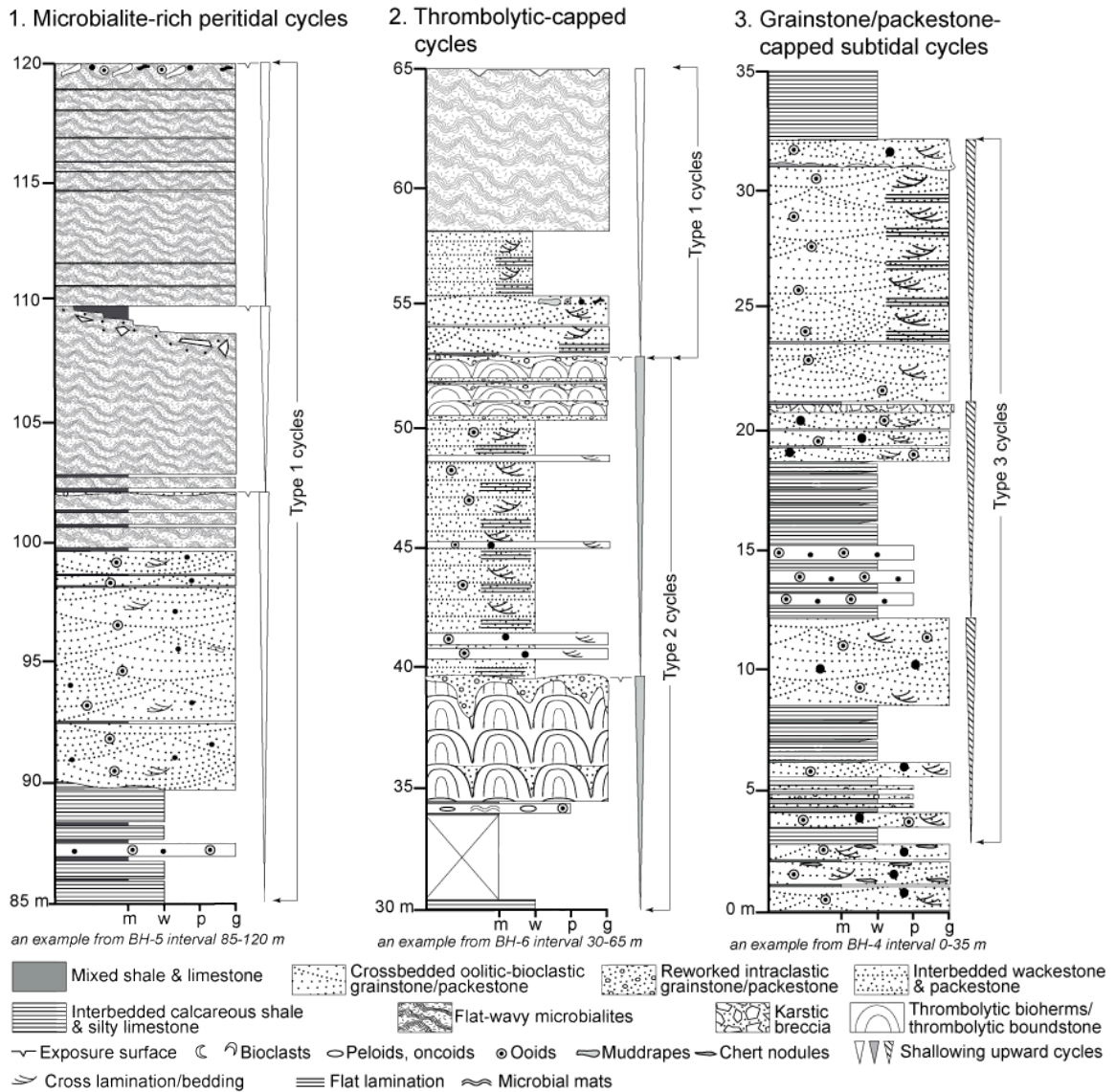


Figure 11. Representative meter-scale cycles from the Big Horse Member of the Orr Formation, Little Horse Canyon, western Utah. Three types of cycles have been identified, including (1) microbialite-rich peritidal cycles, (2) thrombolite-capped peritidal cycles, and (2) grainstone/packstone-capped subtidal cycles. The first two types of cycles are commonly capped by exposure/erosional surfaces, while the subtidal cycles are capped by flooding surfaces expressed by abrupt facies changes. Cycles are identified according to two criteria: the shallowing-upward trend and the bounding surfaces.



Figure 12. Field view of cycles in section BH7. Cycle thickness and component facies in cycles change laterally within walkable distance.

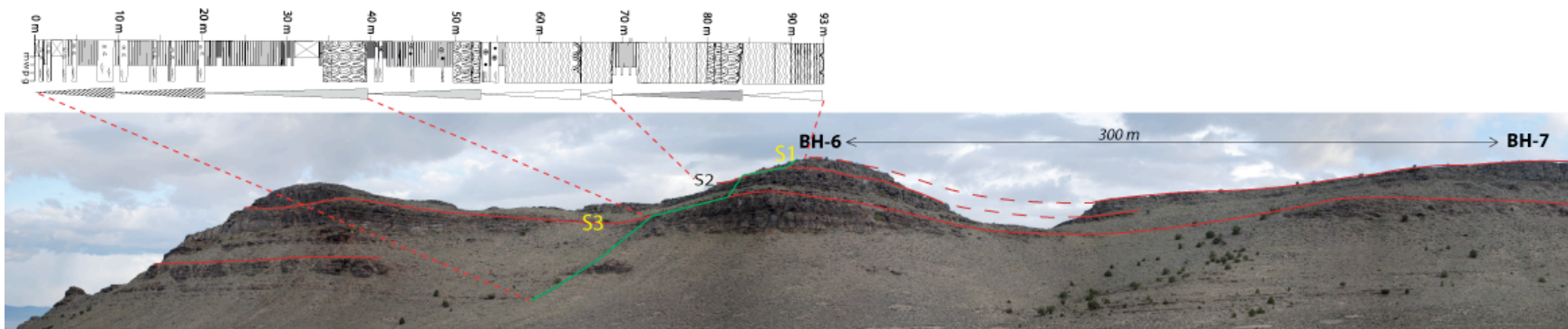


Figure 13. Correlation panel of carbonate cycles in sections BH6 and BH7. The three main surfaces (S1, S2, S3) are traceable from BH-6 to BH-7, but the thickness and facies components are different. The facies below S3 shows a localized thrombolite bioherm.

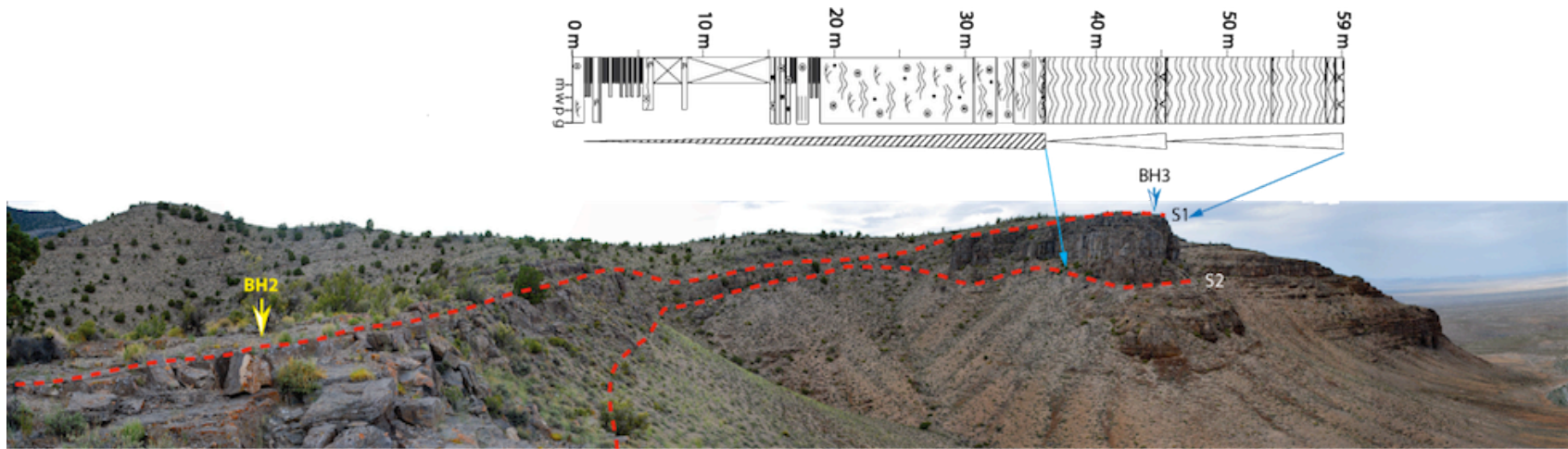


Figure 14. Tracing of carbonate cycles from section BH2 to BH3. The thickness of the interval between S1 and S2 changes significantly over the 250 meter between measured sections.

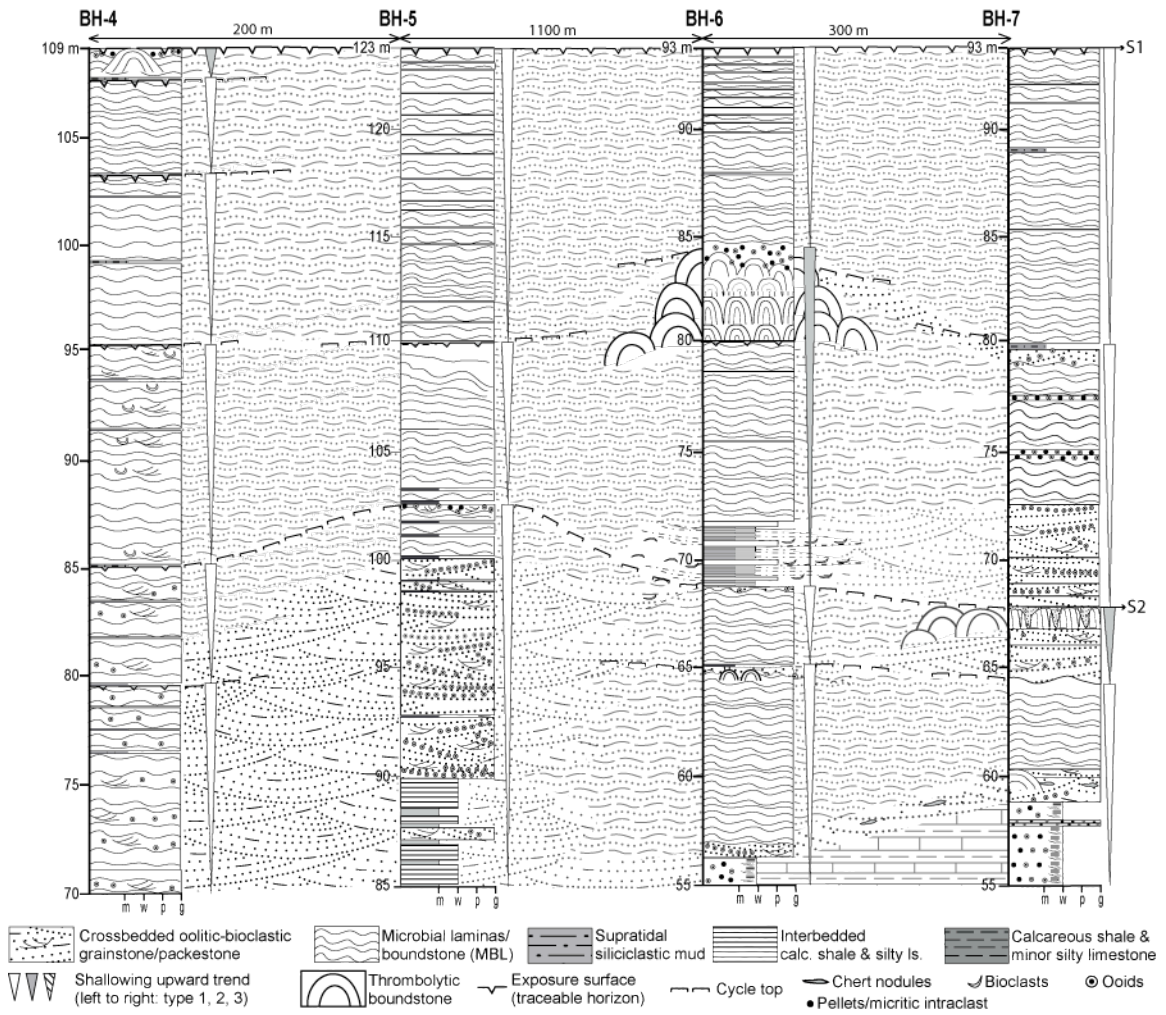


Figure 15. Lateral variability of cycles in the uppermost 40 meters of the studied interval. The number and thickness of cycles change within a few hundred meters from section BH4 to section BH7.

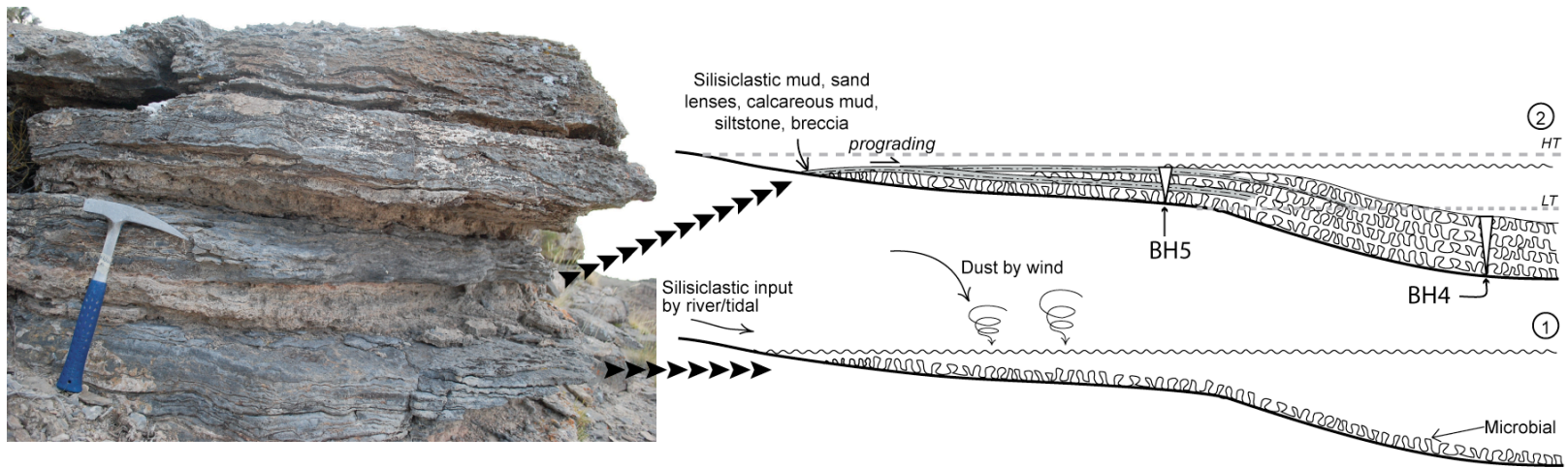


Figure 16. An example showing the formation of microbialite-rich peritidal cycles. Microbial mats occupied the sedimentary substrates in shallow subtidal to intertidal environments, forming flat-wavy microbialites. During the late stage, local subaerial exposure and siliciclastic input forced the migration of the microbial mats. Thus, the upper intertidal facies in section BH5 consists of different internal facies and centimeter-scale cycles, while 200 m away in section BH4, the lower intertidal facies contains only one cycle with homogeneous lithofacies.

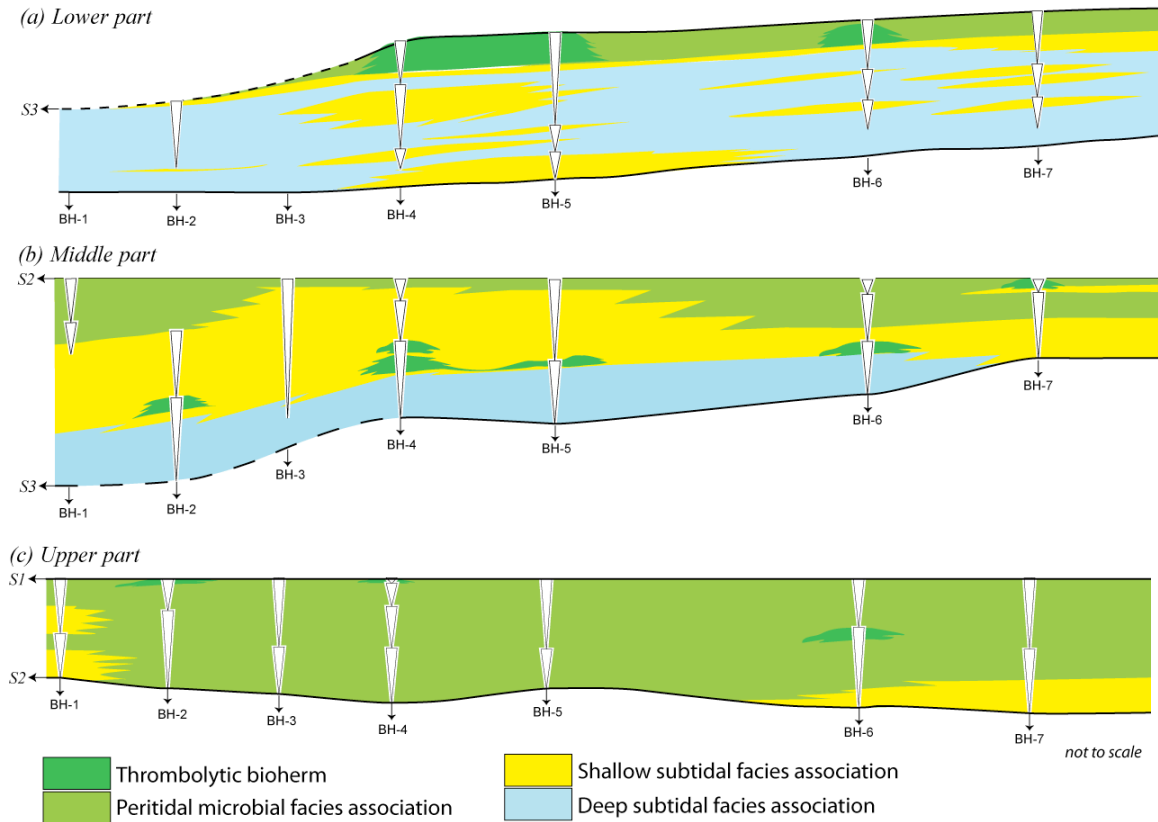


Figure 17. Schematic diagram showing the autogenic origin of cycles and their lateral variations. **(a)** In the lower part (below S3 in Figures 3 and 4) of the measured sections, the depositional environments were subtidal dominated. Local development and migration of shallow subtidal, carbonate sand shoals/bars formed the grainstone/packstone-capped subtidal cycles. At the end of this interval, carbonate sand shoals extended and covered the entire studying area, with local thrombolite bioherms developed at the top. The end of this interval is represented by a karstic surface (S3), indicating the filling of available accommodation space. Subsequent creation of accommodation space is most likely caused by an episode of tectonic subsidence. **(b)** After an episode of tectonic subsidence, the middle part of the studied sections (between S3 and S2) had initial transgression and deepening, but shortly changed to shallow-subtidal-dominated environments. Migration of carbonate sand shoals and local development of thrombolite bioherms created meter-scale cycles that are laterally discontinuous. **(c)** Creation of the accommodation space needed for the deposition of the upper part of the measured sections (between S2 and S1) requires another episode of tectonic subsidence, shortly after the development of surface S2. The background depositional environments representative of this intervals were microbially colonized peritidal environments, within which local development of carbonate sand bars and thrombolite bioherms formed the laterally discontinued cycles.

REFERENCES

- Adams, R.D., and Grotzinger, J.P., 1996, Lateral continuity of facies and parasequences in Middle Cambrian platform carbonates, Carrara Formation, southeastern California, U.S.A: *Journal of Sedimentary Research*, v. 66, p. 1079-1090.
- Berner, R.A., 2003, The long-term carbon cycle, fossil fuels and atmospheric composition: *Nature*, v. 426, p. 323-326.
- Bond, G.C., Kominz, M.A., and Devlin, W.J., 1983, Thermal subsidence and eustasy in the Lower Paleozoic miogeocline of western North America: *Nature*, v. 306, p. 775-779.
- Booler, J., and Tucker, M.E., 2002, Distribution and geometry of facies and early diagenesis; the key to accommodation space variation and sequence stratigraphy; Upper Cretaceous Congost carbonate platform, Spanish Pyrenees: *Sedimentary Geology*, v. 146, p. 225-247.
- Bosence, D., Procter, E., Aurell, M., Kahla, A.B., Boudagher-Fadel, M., Casaglia, F., Cirilli, S., Mehdie, M., Nieto, L., Rey, J., Scherreiks, R., Soussi, M., and Waltham, D., 2009, A dominant tectonic signal in high-frequency, peritidal carbonate cycles? A regional analysis of Liassic Platforms for western Tethys: *Journal of Sedimentary Research*, v. 79, p. 389-415.
- Demicco, R.V. and Spencer, R.J. 1990. Tidal channel, levee, and crevasse-splay deposits from a Cambrian tidal channel system: a new mechanism to produce shallowing-upwards sequence. *Journal of Sedimentary Petrology*, v. 60, p. 73-83.
- Cook, H.E., and Corboy, J.J., 2004, Great Basin Paleozoic carbonate platform: Facies, facies transitions, depositional models, platform architecture, sequence stratigraphy,

- and predictive mineral host models, *in* Open-File Report 2004-1078: United States Geological Survey.
- De Benedicts, D., Bosence, D., Waltham, D., 2007, Tectonic control on peritidal carbonate parasequence formation: An investigation using forward tectono-stratigraphic modeling: *Sedimentology* 54, p. 587-605.
- Dickinson, W.R., 2006, Geotectonic evolution of the Great Basin: *Geosphere*, v. 2, p. 353-368.
- Evans, K.R., 1997, Stratigraphic expression of Middle and Late Cambrian sea-level changes: Examples from Antarctica and the Great Basin, USA [Ph.D. Dissertation]: Lawrence, Kansas, University of Kansas, 177 p.
- Evans, K.R., Miller, J.F., and Dattilo, B.F., 2003, Sequence stratigraphy of the Sauk Sequence: 40th anniversary field trip in western Utah, *in* Swanson, T.W., ed., *Western Cordillera and adjacent areas: Boulder Colorado*, Geological Society of America Field Guide 4, p. 17-35.
- Fischer, A.G., 1964, The lower cyclothems of the Alpine Triassic: *Kansas Geological Survey Bulletin*, v. 169, p. 107-149.
- Goldhammer, R.K., Dunn, P.A., and Hardie, L.A., 1990, Depositional cycles, composite sea-level changes, cycle stacking patterns, and the hierarchy of stratigraphic forcing; examples from Alpine Triassic platform carbonates: *Geological Society of America Bulletin*, v. 102, p. 535-562.
- Goldhammer, R.K., Harris, M.T., Dunn, P.A., and Hardie, L.A., 1993, Sequence stratigraphy and systems tract development of the Latemar Platform, Middle Triassic of the Dolomites (northern Italy); outcrop calibration keyed by cycle stacking

- patterns: AAPG Memoir, v. 57, p. 353-387.
- Grotzinger, J.P., 1986, Cyclicity and paleoenvironmental dynamics, Rocknest Platform, Northwest Canada: Geological Society of America Bulletin, v. 97, p. 1208-1231.
- Hamon, Y., and Merzeraud, G., 2008, Facies architecture and cyclicity in a mosaic carbonate platform effects of fault-block tectonics (Lower Lias, Causes platform, south-east France): Sedimentology, v. 55, p. 155-178.
- Haq, B.U., and Schutter, S.R., 2008, A Chronology of Paleozoic Sea-Level Changes: Science, v. 322, p. 64-68.
- Haq, B.U., Hardenbol, J., and Vail, P.R., 1987, Chronology of fluctuating sea levels since the Triassic: Science, v. 235, p. 1156-1167.
- Hintze, L.F., and Robison, R.A., 1975, Middle Cambrian stratigraphy of the House, Wah Wah, and adjacent ranges in western Utah: Geological Society of American Bulletin, v. 86, p. 881-891.
- Hover-Granath, V.C., Papike, J.J., and Labotka, T.C., 1983, The Notch Peak contact metamorphic aureole: Petrology of the Big Horse Limestone Member of the Orr Formation: Geological Society of America Bulletin, v. 94, p. 889-906.
- Howley, R.A., and Jiang, G., 2010, The Cambrian Drumian carbon isotope excursion (DICE) in the Great Basin, western United States: Palaeogeography, Palaeoclimatology, Palaeoecology, v. 296, p.138-150.
- Jiang, G., Christie-Blick, N., Kaufman, A.J., Banerjee, D.M., and Rai, V., 2002, Sequence stratigraphy of the Neoproterozoic Infra Krol Formation and Krol Group, Lesser Himalaya, India: Journal of Sedimentary Research, vol. 72, p. 524-542

- Jiang, G., Christie-Blick, N., Kaufman, A.J., Banerjee, D.M., and Rai, V., 2003, Carbonate platform growth and cyclicity of a terminal Proterozoic passive margin, Infra Krol Formation and Krol Group, Lesser Himalaya, India: *Sedimentology*, v. 50, p. 921-952.
- Koerschner III, W.F., and Read, J.F., 1989, Field and modeling studies of Cambrian carbonate cycles, Virginia Appalachians: *Journal of Sedimentary Petrology*, v. 9, p. 654-687.
- Kellogg, H.E., 1963, Paleozoic stratigraphy of the southern Egan Range, Nevada: *Geological Society of America*, v. 74, p. 685-708.
- Lehrmann, D.J., and Goldhammer, R.K., 1999, Secular variation in parasequence and facies stacking patterns of platform carbonates: a guide to application of stacking patterns analysis in strata of diverse ages and settings, *Advance in Carbonate Sequence Stratigraphy: Application to Reservoirs, Outcrops, and Models*, SEPM Publication No. 63, p. 187-222.
- Lehrmann, D.J., Donghong, P., Enos, P., Minzoni, M., Ellword, B.B., Orchard, M.J., Jiyang, Z., Jiayong W., Dillet, P., Koenig, J., Steffen, K., Druke, D., Druke, J., Kessel, B., Newkrirk, T., 2007, Impact of differential
- Loucks, R.G., and Sarg, J.F., 1993, Carbonate sequence stratigraphy: AAPG Memoir 57.
- Ludvigsen, R., and Westrop, S.R., 1985, Three new Upper Cambrian stages for North America: *Geology*, v. 13, p. 139-143.
- Lukasik, J.J., and James, N.P., 2003, Deepening-upward subtidal cycles, Murray Basin, south Australia: *Journal of Sedimentary Research*, v. 73, p. 653-671.
- Lukasik, J., and Simo, J.A., 2008, Controls on carbonate platform and reef development:

SEPM Special Publication No. 89.

Mustard, P.S., and Donaldson, J.A., 1990, Paleokarst breccias, calcretes, silcretes and fault talus at the base of Upper Proterozoic "Windermere" Strata, northern Canadian Cordillera, *Journal of Sedimentary Petrology*, v. 60, p. 525-539.

Osleger, D., and Read, J.F., 1991, Relation of eustasy to stacking patterns of meter-scale carbonate cycles, Late Cambrian, U.S.A.: *Journal of Sedimentary petrology*, v. 61, p. 1225-1252.

Palmer, A.R., 1971, The Cambrian of the Great Basin and adjacent areas, western United States, *in* Holland, C.H., ed., *Cambrian of the New World*: London, Wiley-Interscience, p. 1-78.

Pratt, B.R., James, N.P., and Cowan, C.A., 1992, Peritidal carbonates, *in* *Facies Model: Response to sea level changes*, ed., Walker, R.G., and James, N.P.: Geological Association of Canada, p. 303-322.

Pratt, B.R., and James, N.P., 1986, The St George Group (Lower Ordovician) of western Newfoundland: tidal flat island model for carbonate sedimentation in shallow epeiric seas: *Sedimentology*, v. 33, p. 313-343.

Rees, M.N., 1986, A fault-controlled trough through a carbonate platform: the Middle Cambrian House Range embayment: *Geological Society of America Bulletin*, v. 97, p. 1054-1069.

Rees, M.N., and Robison, R.A., 1989, Cambrian stratigraphy and paleontology of the central House Range and Drum Mountains, Utah, *American Geophysical Union*, v. T125, p. 59-72.

Riding, R., 2000, Microbial carbonates: the geological record of calcified bacterial-algal

- mats and biofilms: *Sedimentology*, v. 47, p. 179-214.
- Saltzman, M.R., Runnegar, B., and Lohmann, K.C., 1998, Carbon isotope stratigraphy of Upper Cambrian (Steptoean Stage) sequences of the eastern Great basin: Record of a global oceanographic event: *Geological Society of America Bulletin*, v. 110, p. 285-297.
- Sami, T.T., and James, N.P., 1994, Peritidal carbonate platform growth and cyclicity in an early Proterozoic foreland basin, Upper Pethei Group, northwest Canada: *Journal of Sedimentary Research*, v. B64,
- Sarg, J.F., Markello, J.R., Weber, L.J., 1999, The second-order cycle, carbonate-platform growth, and reservoir, source, and trap prediction, *Advance in Carbonate Sequence Stratigraphy: Application to Reservoirs, Outcrops, and Models*, SEPM Publication No. 63, p. 187-222.
- Soreghan, G.S., and Dickinson, W.R., 1994, Generic types of stratigraphic cycles controlled by eustasy: *Geology*, v. 22, p.759-761.
- Spence, G.H., and Tucker, M.E., 2007, A proposed integrated multi-signature model for peritidal cycles in carbonates: *Journal of Sedimentary Research*, v. 77, p. 797-808.
- Tucker, M.E. and V.P. Wright, 1990, *Carbonate Sedimentology*: Oxford: Blackwell Scientific Publications, 482 p.

VITA

Graduate College
University of Nevada, Las Vegas

Ratna Widiarti

Degrees:

Bachelor of Science, Geology, 2008
Institute of Technology Bandung, Indonesia

Publications:

Widiarti, R., and Jiang, G., 2010, Carbonate cycle and their controlling mechanism during late Cambrian greenhouse time in central Nevada and western Utah: American Association of Petroleum Geologists, Abstract with Programs of Annual Convention and Exhibition 2010.

Widiarti, R., and Noeradi, D., 2008, Reservoir modeling of shallow part reservoir in the Handil Field, Mahakam Delta: Indonesia Petroleum Association Annual Convention 2008.

Thesis Title: Lateral Variability of Facies and Cycles in the Furongian (Late Cambrian) Carbonate Platform: An Example from the Big Horse Member of the Orr Formation in Western Utah, U.S.A.

Thesis Examination Committee:

Chairperson, Ganqing Jiang, Ph.D
Committee Member, Stephen M. Rowland, Ph.D
Committee Member, Andrew D. Hanson, Ph.D
Graduate Faculty Representative, Felicia F. Campbell, Ph.D